TECHNICAL REPORT STANDARD TITLE PAGE

1. REPORT NO.	2. GOVERNMENT ACCESSION NO.	3. RECIPIENT'S CATALOG NO.
WA-RD 406.2		

4. TITLE AND SUBTITLE	5. REPORT DATE
Determination of Rheological Parameters of Pile Foundations for Bridges for Earthquake Analysis	July 1997
	6. PERFORMING ORGANIZATION CODE
7. AUTHOR(S)	8. PERFORMING ORGANIZATION REPORT NO.
William F. Cofer and Sukomal Modak	
9. PERFORMING ORGANIZATION NAME AND ADDRESS	10. WORK UNIT NO.
Washington State Transportation Center (TRAC) Civil and Environmental Engineering; Sloan Hall, Room 101 Washington State University Pullman, Washington 99164-2910	11. CONTRACT OR GRANT NO. T9234-07
12. SPONSORING AGENCY NAME AND ADDRESS	13. TYPE OF REPORT AND PERIOD COVERED
Washington State Department of Transportation Transportation Building, MS 7370 Olympia, Washington 98504-7370	Summary Report
	14. SPONSORING AGENCY CODE

15. SUPPLEMENTARY NOTES

This study was conducted in cooperation with the U.S. Department of Transportation, Federal Highway Administration.

16. ABSTRACT

In the seismic design criteria for highway bridges, there is a significant lack of guidance on ways to incorporate the effect of soil-structure interaction in determining seismic response. For this study, a simple analytical model for pile and pile group foundations is presented for use in dynamic modeling of bridge superstructures. Both the axial and lateral pile response is considered. This simple model consists of a set of nonlinear springs, dampers, and masses for each degree-of-freedom of the pile, and it is based on the Winkler hypothesis. The spring behavior was established by using the finite element method for static load conditions and a typical soil from Washington State. The lumped damping constants and masses were based on realistic approximations. The *p-y* and *t-z* curves for single piles and two-pile groups were presented for two pile diameters. Using these curves as near-field Winkler elements, combined with established far-field elements, the dynamic response of a single pile when subjected to a half-sine impulse load was compared to that of a more rigorous, nonlinear, three-dimensional finite element analysis. Close agreement was observed. For design, suggestions were made on ways to develop an approximately equivalent foundation model consisting of a single mass, spring, and damper.

17. KEY WORDS	18. DISTRIBUTION STATEMENT
Key words: bridge, earthquake, pile, group, finite element	No restrictions. This document is available to the public through the National Technical Information Service, Springfield, VA 22616

19. SECURITY CLASSIF. (of this report)	20. SECURITY CLASSIF. (of this page)	21. NO. OF PAGES	22. PRICE
None	None	49	

Summary Report
for
Research Project T9234-07
"Modeling Pile Foundations for Seismic Analysis"

Determination of Rheological Parameters of Pile Foundations for Bridges for Earthquake Analysis

by

William F. Cofer and Sukomal Modak
Washington State Transportation Center (TRAC)
Washington State University
Department of Civil & Environmental Engineering
Pullman, WA 99164-2910

Washington State Department of Transportation
Project Manager
Keith Anderson

Prepared for

Washington State Transportation Commission
Department of Transportation
and in cooperation with
U.S. Department of Transportation
Federal Highway Administration

July 1997

DISCLAIMER

The contents of this report reflect the views of the authors, who are responsible for the facts and the accuracy of the data presented herein. The contents do not necessarily reflect the official views or policies of the Washington State Transportation Commission, Department of Transportation, or the Federal Highway Administration. This report does not constitute a standard, specification, or regulation.

TABLE OF CONTENTS

Section	Page
Executive Summary	1
Introduction	3
Problem Statement	3
Soil-Structure Interaction	3
Objectives	5
Review of Previous Work	6
Literature Review	6
Research Approach	10
Modeling of a Single Pile	11
Lateral Vibration of a Single Pile	11
Axial Vibration of a Single Pile	22
Modeling of Pile Groups	28
Characteristics of Springs in Two-Pile Groups	29
Pile Cap Behavior	36
Pile Tip Behavior	37
Findings	37
Lateral Response of a Single Pile	37
Conclusions	42
Implementation	42
References	47

LIST OF FIGURES

Figure		Page
1.	A model for lateral vibration of single pile	12
2.	Finite element mesh used for the analysis of 2D soil-pile layer for lateral vibration of single pile. Symmetry has been used	13
3.	A typical *p-y* curve for the near-field spring, shown as lateral force per length of pile (pounds/inch) versus displacement (inches)	15
4.	A pile leaves a gap behind it when plastic deformation continues during lateral motion	15
5.	A linearized idealization of *p-y* curves	17
6.	A model for axial vibration of single pile	23
7.	Finite element mesh used for the analysis of 2D soil-pile layer for axial vibration of single pile	24
8.	Model for direct-lateral vibration of a two-pile group moving laterally along the line which passes through the piles	29
9.	A more general model for vibration of a two pile group for direct-lateral and shear-lateral vibration	30
10.	Finite element mesh used for the analysis of 2D pile-soil-pile layer	32
11.	Concept of tributary area employed to find approximate mass contributions from soil to the piles in a pile group	34
12.	The FEM model used for the analysis of lateral vibration of a single pile	38
13.	The lumped models used for the analysis of lateral vibration of a single pile	39
14.	The load history used to analyze the lateral vibration of the single pile	41
15.	The pile head displacement histories obtained from the discrete model	41
16.	Pile head response, 50 kip lateral load at 1 hz	45
17.	Pile head response, 50 kip lateral load at 2 hz	45
18.	Pile head response, 100 kip lateral load at 1 hz	46
19.	Pile head response, 100 kip lateral load at 2 hz	46

LIST OF TABLES

Table		Page
1.	NEABS parameters for *p-y* curves for a single pile vibrating laterally for different confining pressures. [d = 18 in, K'_o = 0.50, f = 0.40, isotropic hardening, drained condition]	18
2.	NEABS parameters for *p-y* curves for a single pile vibrating laterally for different confining pressures. [d = 24 in, K'_o = 0.50, f = 0.40, isotropic hardening, drained condition]	18
3.	NEABS parameters for *t-z* curves for single pile vibrating axially for different confining pressures. [d = 18 in., K'_o = 0.50, isotropic hardening, drained condition]	26
4.	NEABS parameters for *t-z* curves for single pile vibrating axially for different confining pressures. [d = 24 in., K'_o = 0.50, isotropic hardening, drained condition]	26
5.	Pile response data and equivalent properties for the single pile model	44

EXECUTIVE SUMMARY

Current seismic design criteria for highway bridges generally require that the effects of earthquake loading be evaluated using either an equivalent static load approach for simple bridges or a dynamic analysis for more complex bridges. These provisions usually provide detailed explanations and commentaries on techniques which are judged to be suitable for static and dynamic modeling of the bridge superstructure and supporting columns or piers. There is, however, a significant lack of guidance on exactly how the boundary conditions and soil-structure interaction should be incorporated into the model.

The purpose of this study is to present a simple analytical model of pile and pile group foundations for use as boundary conditions in a numerical model for seismic analysis of highway bridges. Both the axial and lateral response are considered. This simple model consists of a set of springs, dampers, and masses for each degree-of-freedom on the pile, and it is based upon the Winkler hypothesis. The spring behavior is established by using the finite element method for static load conditions. The lumped damper constants and masses are based on realistic approximations. The effect of a sliding interface, nonlinearity of the soil, and geometric, hysteresis, and viscous damping of the soil have been considered.

The *p-y* and *t*-z curves for lateral and axial vibration of single piles of 18-inch (0.457 m) and 24-inch (0.610 m) diameter based on two-dimensional analysis for different depths have been presented for a typical soil from Washington State. Similar curves for direct-lateral, shear-lateral, and axial vibration interaction have also been presented for two-pile groups with different spacings.

Using these *p-y* and *t-z* curves as near-field Winkler elements, combined with far-field Winkler elements from the literature, the dynamic response of a single pile when subjected to a half-sine impulse load was compared to that of a more rigorous, nonlinear, three-dimensional finite element analysis. Close agreement was observed, justifying the use of the simplified model. For design, suggestions were made on ways to develop an

approximately equivalent foundation model consisting of a single spring, mass, and damper.

INTRODUCTION

PROBLEM STATEMENT

Highway bridges have suffered extensive damage in recent earthquakes. Much of the damage has been caused by excessive forces at supports and by weakness of the substructure. For most bridge design codes, the dynamic effects of the ground motion are either expressed as a set of equivalent lateral static forces which are proportional to the weight of the superstructure or obtained through a linear modal analysis. For the latter, the structure is assumed to remain fully elastic and the supports are considered to be either simply supported, fully fixed, or expressed as a set of linear springs. Energy dissipation is included through the use of proportional damping in which a uniform damping coefficient is applied for each mode shape. A linear analysis for a design earthquake is then performed in either the frequency or time domain. Any nonlinearities that arise in the foundations are included in an iterative fashion, by which a secant stiffness is defined on the basis of the maximum foundation displacement.

However, more elaborate procedures are justified for structures of major importance or if soil-structure interaction is of definite consequence in design. In this case, techniques that might be considered include better estimates of soil properties and foundation stiffness, mass, and damping characteristics. The analysis method should take into account the nonlinear effects of both the structure and the supporting medium. Recently, software has been developed for bridge analysis that can include the concentrated mass, damping, and nonlinear stiffness properties for nonlinear foundations (Cofer, et al. 1994). However, procedures to obtain these properties for pile foundations and then accurately and economically model their dynamic effects are not well developed.

SOIL-STRUCTURE INTERACTION

Soil-structure interaction refers to the effect that the founding soil has on the dynamic response of a structure and, conversely, the effect of the structure on the soil motion. The influence on the structural response often includes an amplification of the

translational motion, the introduction of a rocking component for an embedded foundation, an increase in the flexibility of the system, and the addition of damping from hysteretic action of the soil (hysteretic damping) and radiation of energy away from the structure in the form of outward-propagating soil waves (radiation damping).

Two general approaches are available for rationally incorporating soil-structure interaction effects into structural analysis (Wolf 1985). In the direct method, the structure and a portion of the founding soil are both incorporated into a finite element mesh. This is the simplest approach conceptually, but a number of drawbacks, including the need for a large model, energy absorbing boundaries, and detailed soil properties, make its use prohibitive for all but the most extreme analysis demands.

A simpler, more efficient approach is the substructure method. Here, the structure and the soil are analyzed separately. A simplified model is constructed that can approximate the behavior of the soil at the foundation. This simplified model is then coupled with the structure at the supports, and the structure is analyzed.

The foundation model is typically composed of one or more springs or spring/mass/damper combinations arranged in series or parallel for each degree-of-freedom. They are chosen on the basis of the assumed foundation behavior, which is obtained either experimentally or analytically.

The most common analytical model is one in which the soil domain is considered to be a homogeneous, elastic half-space. The frequency domain solution for the dynamic response of a rigid disk on an elastic half-space has been derived and extended for footings of various other shapes and depths of embedment. One should note that the disk/half-space solution is frequency dependent. For nonlinear analysis, which must be conducted in the time domain, various foundation models have been proposed that reproduce the analytical foundation response for certain ranges of loading frequencies. Several such models were evaluated in an earlier report (Cofer, et al. 1994), in which it was noted that a simple spring/mass/damper model performed adequately in comparison with more complex models.

Because half-space solutions are only available for structures resting on the ground surface, there is no simple means for determining spring constants and dampers for embedded structures. Spring constants for embedded structures can be determined with reasonable accuracy by static finite element analyses, but damping characteristics cannot be found from a static analysis. More frequently, standard formulas are used, even though they are not strictly valid for embedded structures and they become increasingly invalid with increasing depth of embedment. Also, for embedded structures, substructure analyses are invariably based on the assumption that motions around the structure are the same as those below the base; i.e., the motions are everywhere the same in the surrounding soil. However, there is much evidence to show that ground motions vary considerably with depth during earthquakes. Therefore, there is a need for research to clarify the behavior of piles when subjected to seismic loading and to develop suitable simplified models for seismic analysis.

OBJECTIVES

The aim of the research reported herein is to develop a rational, dynamic, lumped-parameter soil-pile interaction model for both lateral and axial vibration of single piles and pile groups. The specific objectives are as follows:

1. Obtain equivalent stiffness properties for single piles and pile groups that can be used to model the nonlinear behavior of pile foundations for the seismic analysis of bridge superstructures;
2. Obtain equivalent damping properties for piles and pile groups, including contributions from radiation, viscous, and hysteretic damping in foundation soil;
3. Obtain lumped mass properties for piles and pile groups;
4. Define the dynamic pile interaction effects for groups of two piles; and
5. Suggest simplified modeling procedures to include the effect of pile foundations in the seismic analysis of bridges.

REVIEW OF PREVIOUS WORK

LITERATURE REVIEW

Techniques for the analysis and design of pile foundations have evolved rapidly over the past three decades from completely empirical methods to numerical approaches which are derived on a more solid theoretical basis. Important effects that must be considered for analysis include nonlinear soil constitutive properties, the interface properties between the pile and the soil, and the influence of group behavior. For dynamic analysis, additional considerations include the degradation of soil stiffness under cyclic loading, loading rate effects, and the accumulation of permanent displacements (Poulos 1989). So many papers have been published on pile dynamics that it is impossible to mention all of them in this report. For a more complete discussion, the reader is referred to the Technical Report (Cofer, et al. 1996).

The simplest approach for computing the response of piles is the Winkler method in which the pile is modeled with standard linear elastic beam elements and the soil is represented as a distributed elastic stiffness which depends upon soil properties and the radius of the pile. The most straightforward approach to determine the value of the distributed stiffness is to assume that the soil is an elastic half-space. Typically, either Mindlin's displacement field in an elastic half-space is used to compute flexibility coefficients which may then be inverted to obtain stiffness values (Poulos 1989) or the Boundary Element Method is used (Mamoon and Banerjee 1990). Pile-soil slippage and separation are not included in these elastic analyses (Trochanis, et al. 1991a). The effect of the pile diameter is ignored, as well, because the pile is idealized as an infinitely thin strip when computing the soil stiffness (Randolph 1981).

As a simplification, the distributed soil stiffness may be modeled as a series of discrete springs, called the load-transfer analysis (Poulos 1989), for which the soil deflection at a point is uncoupled from the response at other points. Closed form solutions are available and are of a particularly simple form for long piles (Randolph 1981).

Soil nonhomogeneity and material nonlinearities may be included fairly easily in the load-transfer analysis. Penzien (1970) used a discrete model to perform a seismic analysis of a bridge that was founded on piles driven through soft soil. The mass of the piles and the effective mass of the soil were lumped and the soil stiffness was included through discrete bilinear spring/viscous damper elements. More recently, the nonlinear load-deformation behavior of the soil springs for the static analysis of individual offshore pile foundations has been defined by so-called *p-y* curves, developed empirically for several soil types. A dynamic analysis of two cable-stayed bridges in which *p-y* curves were used to include the near-field behavior of soil around piles was reported by Elassaly, et al (1995). Obtaining the appropriate properties for a specific pile size and soil type involves a certain amount of engineering judgement, however (Leung and Chow 1987).

In order to model far-field stiffness and radiation damping effects on the dynamic behavior of piles, Nogami and Konagai (1988) represented the soil as a vertically-stratified series of plane-strain elastic layers to develop discrete spring/mass/damper models for use in a load-transfer analysis. The authors report that this model accurately reproduces the behavior of the plane-strain elastic half-space over a wide frequency range.

The concept was later extended (Nogami, et al. 1992) to include in the soil reaction model a nonlinear near-field sub-model, and a sub-model capable of representing the development of a gap between the pile shaft and the soil. These sub-models are intended to be placed in series with the previously derived far-field element in order to represent the nonlinear, hysteretic action of the soil in the immediate vicinity of the pile.

In practice, piles are often arranged in groups and the pile-soil-pile interaction becomes significant as the distance between the piles decreases. These group effects increase the overall settlement, redistribute the loads on individual piles, and modify group stiffness and damping properties (El Sharnouby and Novak 1985). The significance and complexity of these pile-soil-pile interaction effects have been shown to be more pronounced for dynamic loading than for static loading (Nogami 1985).

Makris, et al (1992), performed a dynamic analysis of a bridge for which the soil-pile-structure interaction for groups of 20 piles was included through the use of simple formulas for foundation impedances. However, the use of frequency dependent impedances implies that only linear analysis can be performed. Although the predicted response was similar to recorded motions from the site, the deck acceleration response was underestimated by 30 percent, suggesting that a nonlinear analysis would be more realistic.

However, the load-transfer method cannot be used directly to model pile-soil-pile interaction because the soil continuum must be included in the analysis. Mindlin's equations (Poulos 1989; El Sharnouby and Novak 1985; Leung and Chow 1987) and the Boundary Element Method (Mamoon and Banerjee 1990) have been used to obtain the influence of one pile upon another. Several methods for analyzing pile groups have then been applied (Poulos, 1989), including the complete analysis of the group, a hybrid method in which a load-transfer analysis is used to obtain the response of each pile and continuum theory is applied to include the influence of other piles, and the use of two-pile analyses to define interaction factors between each set of piles in the group.

The Finite Element Method has been applied for the analysis of piles and pile groups. Ottaviani (1975) modeled pile groups in a three dimensional analysis that also included an embedded cap. The soil was a homogeneous, linearly elastic continuum and no relative displacements were allowed between the cap, the piles, and the soil. A similar analysis has been reported by Randolph (1981) for the lateral response of single cylindrical piles in elastic soil with stiffness varying linearly with depth.

Jardine, et al (1986), considered the axisymmetric, two dimensional analysis of a single pile, along with other types of foundations, to study the influence of nonlinear material properties on soil-structure interaction. Pressley and Poulos (1986) performed an equivalent axisymmetric finite element analysis of a pile group which considered elastic-plastic soil behavior and slip at the pile-soil interfaces. A similar nonlinear analysis, but in three dimensions, was reported by Muqtadir and Desai (1986). This

study demonstrated that the consideration of soil nonlinearity and interface effects significantly influenced the behavior of the pile group.

Trochanis, et al (1991a), used the dynamic finite element software, DYNA3D, to perform three dimensional analyses of single piles and two-pile groups for the purpose of examining the effect of nonlinearities on their response to monotonic and cyclic (pseudodynamic) loading. Drucker-Praeger elastic-plastic continuum elements were used to model the soil and interface elements were included to allow slipping and separation between the piles and the soil. The piles themselves were modeled with square cross sections and the loads were applied to the pile heads. The authors concluded that the interaction between piles is markedly reduced as a result of pile-soil interface effects. A similar analysis was performed by Brown and Shie (1990) for a single pile subjected to static lateral loading. Solid elements with curved sides were used to represent the circular cross section of the pile and the analyses were used to provide a basis for future parametric studies.

The use of the Finite Element Method in three dimensions for the analysis of piles and pile groups has several advantages over the elastic half-space approach in that the effects of the pile diameter, soil-pile slippage and gap formation, nonhomogeneous soil, and nonlinear soil properties may be included in a straightforward way. In addition, a complete history of stresses, deformations, moments, and forces for the entire cap-pile-soil system is available. However, this type of analysis is cumbersome for routine pile design. Nogami (1985) has shown that the load-transfer method can provide pile group responses that are close to those obtained through other, more rigorous models if appropriate stiffness values are chosen for the discrete springs. Pile-soil-pile interaction effects were included through additional discrete springs that connected adjacent piles. The stiffness for these springs was obtained through a dynamic, plane strain analysis in which two pile cross sections were modeled within an elastic soil layer of unit thickness. In further research (Nogami and Konagai 1987), the nonlinear effects from pile-soil slippage were added.

Bown and Shie (1990) used several types of finite element analyses to obtain *p-y* curves for a single pile subjected to static loading. They noted that, even for homogeneous soil, the behavior of the soil in the nonlinear range varies with depth as a result of surface effects. Two dimensional plane stress and plane strain analyses were shown to provide upper and lower bounds to the curves obtained through the more detailed three dimensional model.

Trochanis, et al (1991b), also used their nonlinear, three dimensional finite element analyses of pile groups to define a simplified load-transfer model. The nonlinear response due to soil yielding and pile-soil slippage and separation were included through a degrading hysteretic spring model. Close agreement was observed between the behavior of the simplified model and that of the three dimensional study.

RESEARCH APPROACH

In order to accomplish the objectives of this research, the Finite Element Method was used to obtain the equivalent dynamic properties for discrete spring/mass/damper elements to be applied to a load transfer model for pile foundations. The results of the load transfer model when subjected to a dynamic loading were then compared to those of a full three dimensional finite element model of the pile and surrounding soil to verify its modeling capabilities. A method was then proposed to use the load transfer model to obtain a simplified spring/mass/damper representation for the entire foundation that can be applied to the dynamic analysis of a bridge superstructure, including, in a rational way, soil structure interaction effects.

Circular piles of 18 in. (457 mm) and 24 in. (610 mm) diameter were considered for a typical soil from Washington State. The far-field representation for a disk in a plane-strain elastic layer was used to define the dynamic far-field properties in accordance with the derivation of Nogami and Konagai (1988). Several two dimensional finite element models that included cross sections of single piles, sets of two piles at various

spacings, and typical pile cap models were analyzed with pseudo-static harmonic loads to obtain near-field properties.

DYNA3D, a nonlinear, finite deformation finite element code for dynamic analysis in three dimensions was used for these analyses. Isoparametric solid elements with single point integration and hourglass control were used to model both the soil and the pile cross sections. The piles were modeled as rigid disks for 2-D models and assumed to be linearly elastic for 3-D models, while soil was assumed to be elasto-plastic. The plastic behavior was represented using the Geologic Cap Model. For this material model, the failure envelope consists of a yield function which is based upon both the second invariant of deviatoric stress and the pressure, a hardening cap surface, and a tension cutoff surface. The pile-soil interfaces were modeled by using slidelines which permit sliding with separation, closure, and friction.

MODELING OF A SINGLE PILE

For modeling a single pile, the model proposed by Nogami et al. (1992) for lateral vibration and that proposed by Nogami and Konagai (1986, 1987, 1988) for axial vibration were applied with some modification.

Lateral Vibration of a Single Pile

For lateral vibration, the pile was modeled as a beam on inelastic Winkler-type foundation modified for dynamic analysis. It is based on a thin layer solution. In this model, there are two nodes at each layer: a pile node and an auxiliary node. The model consists of a nonlinear near-field spring, a linear near-field viscous damper, lumped masses at the pile and auxiliary nodes, three linear far-field springs, and three linear far-field dampers. The model is shown in Figure 1. Nogami et al. (1992) has provided explicit expressions for the far-field element parameters in terms of elastic soil properties. In this report, the major emphasis is on the formulation of the nonlinear near-field springs and the lumped masses.

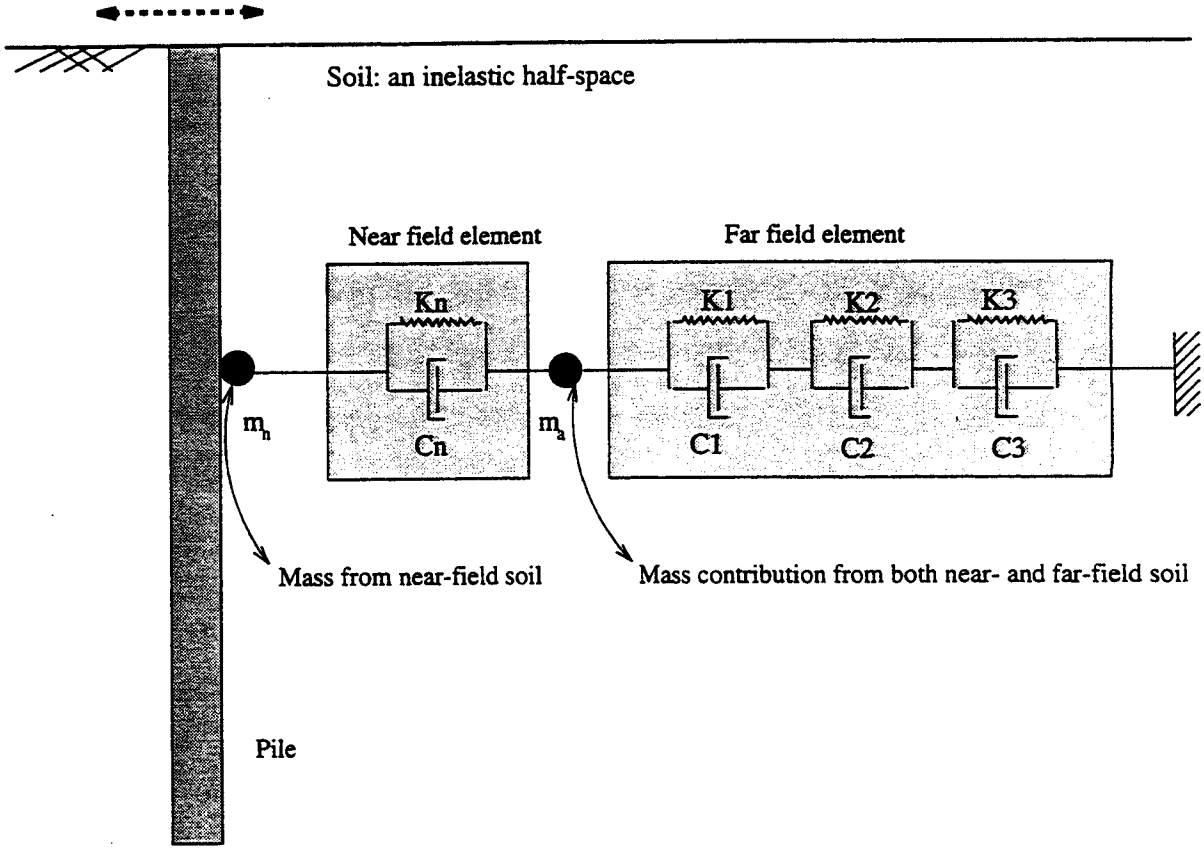

Figure 1. A model for lateral vibration of single pile.

Near-Field Spring

The near-field spring properties were obtained on the basis of finite element analysis of a circular thin soil layer of unit thickness and diameter $40d$, where d is the diameter of the pile. Within the range of stress developed, it was assumed that the pile segment is relatively rigid. Therefore, the pile was modeled as a rigid disk, surrounded by a mesh representing the soil, as shown in Figure 2. Soil within a radius of $4d$ from the pile center was modeled with the geologic cap material model. The remainder of the soil was modeled with consistent elastic properties because soil strains are assumed to be small away from the pile. All parameters for modeling of the soil properties were appropriate for the depth considered and for the existing K_o-stress condition. The initialization of geo-static stress was done by incorporating the initial stress output file from the implicit

finite element companion program, NIKE3D. A sliding interface was also included to model gap formation, impact within a gap, and sliding with friction.

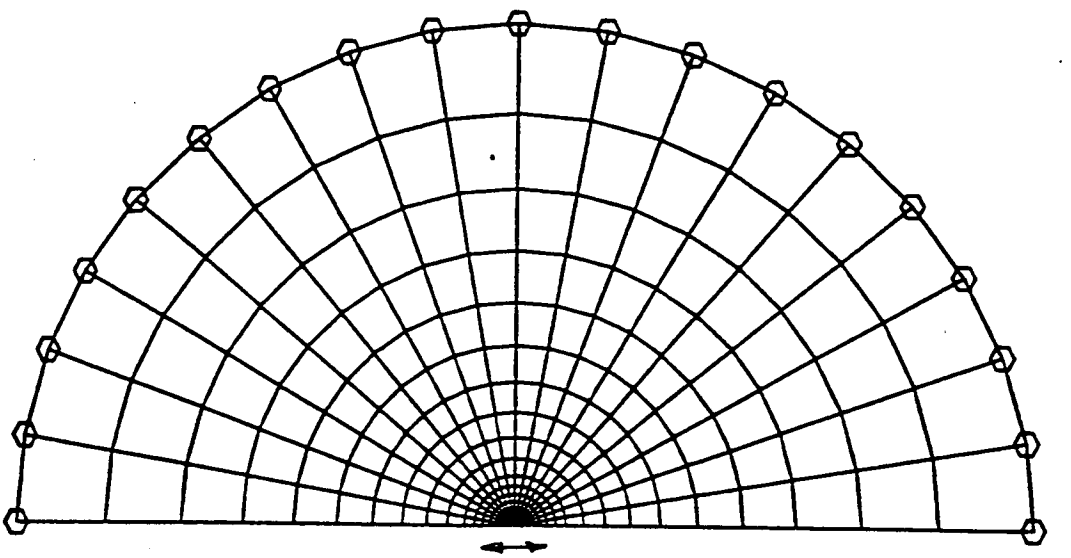

Figure 2. Finite element mesh used for the analysis of 2D soil-pile layer for lateral vibration of single pile. Symmetry has been used.

Plane strain analyses for several depths of soil representing vertical effective stress values of 1, 2.5, 5, 10, 20, 40, 80, and 160 psi (6.9, 17.3, 34.5, 68.9, 137.8, 275.6, 551.2, and 1102.4 kPa) were performed. However, for very small depths, the plane stress condition was assumed to be most appropriate, and plane stress analyses were performed for vertical effective stress values of 1, 2.5, 5, and 10 psi (6.9, 17.3, 34.5, and 68.9). The soil parameters and the resulting cap model parameters are tabulated in the Technical Report (Cofer et al. 1996).

To develop the nonlinear near-field spring, the pile segment was forced to move laterally either in the plane stress or plane strain condition during the computer simulation

of a lateral load test. The finite element mesh is shown in Figure 2 and the displacement of the segment was monitored. The lateral force-displacement behavior is represented by *p-y* curves, in which *p* is lateral force per unit length of pile and *y* is lateral displacement. A typical *p-y* curve is shown in Figure 3 for two cycles of the load, and it includes nonlinearities from hysteretic and gap behavior.

Initially, when a pile segment moves laterally in a thin layer of soil, the force-displacement relationship remains linearly elastic. When the force level exceeds the elastic range, the pile leaves a gap behind it and plastic deformation continues, as shown in Figure 4. The slope of the *p-y* curve changes to represent plastic behavior. Upon unloading, the pile segment moves back elastically until the 'zero' force state is almost reached. Then, with reverse loading, the pile moves back, through the gap created before, with very small resistance. Here, the slope of the *p-y* curve is called the *first gap stiffness*. With increasing reverse load, the pile segment reaches the rear end of the gap, after which the loading behavior is elastic until reverse plastic loading occurs. The slope of reverse plastic loading is similar to that of the loading elasto-plastic slope. At the same time, the rear end of the gap moves more. Reverse loading becomes elastic again until the 'zero' force state is again reached. Then, the pile moves back through the gap.

A comprehensive determination of near-field spring constants has been made for piles with diameters of 18 in. (457 mm) and 24 in. (610 mm), respectively, using soil parameters determined from laboratory tests performed on soil samples taken from a Snohomish River site in Washington State. Most of the soil samples were silty (MH, ML, SM). The soil was uniform from depths of 10 ft. (3 m) to 30 ft. (9 m). Constant soil parameters for this range of depths were used, with modification for confining pressures. These thin-layer *p-y* curves were produced, assuming drained conditions. In all cases, the coefficient of earth pressure at rest, K_o, was assumed to be 0.5, and the coefficient of friction in the interface was assumed to be 0.4. The *p-y* curves for very small vertical stress were developed for the plane stress condition. All *p-y* curves are presented in the Technical Report (Cofer et al. 1996).

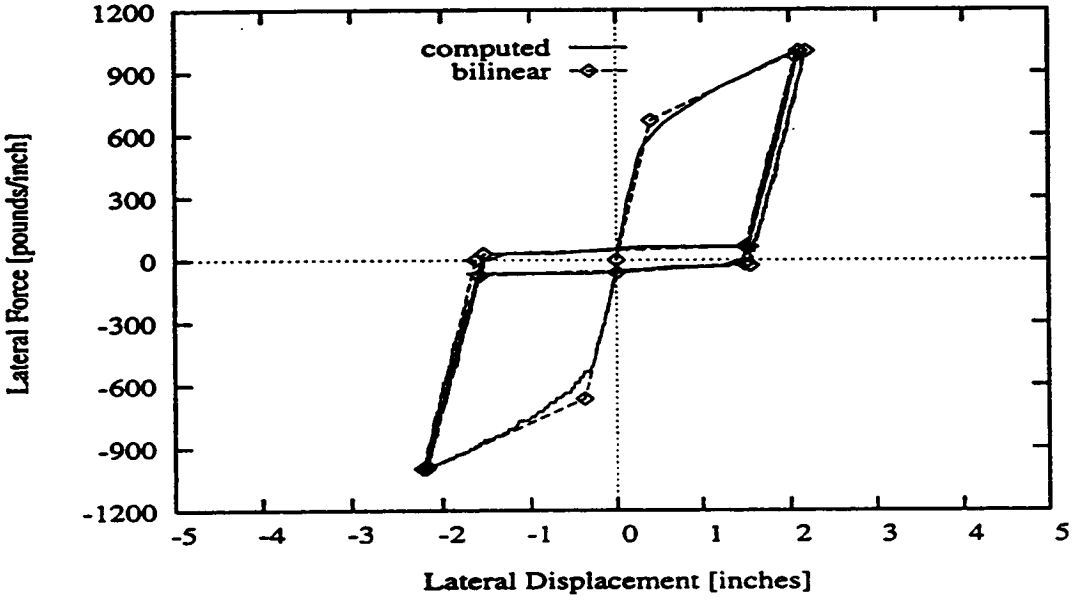

Figure 3. A typical *p-y* curve for the near-field spring, shown as lateral force per length of pile (pounds/inch) versus displacement (inches).

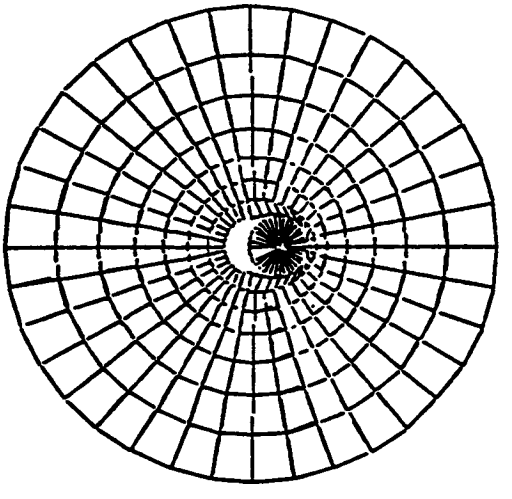

Figure 4. A pile leaves a gap behind it when plastic deformation continues during lateral motion.

For the analysis of pile vibration using the NEABS program, as modified by McGuire (1993), the *p-y* curve must be simplified as a combination of several linear segments with: (1) initial stiffness, K_1; (2) yield force, F_y; (3) hardening stiffness without gap, K_2; (4) unloading stiffness without gap, K_3; (5) hardening stiffness with gap, K_4; (6) unloading stiffness with gap, K_5; (7) hardening parameter, β; and (8) a gap parameter representing the capability of the trailing edge to follow the leading edge of the gap, γ. Figure 5 shows the idealized *p-y* curve.

The parameters K_1 and K_3 are found to be more or less the same for all of the *p-y* curves. Also, K_5 cannot be determined from a load controlled test. Its value has a minor significance in practice, and should be between K_4 and K_1. K_5 can be taken to be equal to K_1. The hardening parameter, β, represents the way in which the *p-y* curve hardens for reverse loading with elasto-plastic load increments. For isotropic hardening, β equals one, and for kinematic hardening, β equals zero. Intermediate values of β represent mixed hardening. The gap parameter, γ, represents the behavior of the movement of the leading and trailing edges of the gap. Effectively, it relates the plastic movement of soil, $u_{plastic}$ and the generated gap, u_{gap}.

$$\gamma = \frac{u_{gap}}{u_{plastic}}$$

Figure 3 shows the matching between the *p-y* curve and its linearized version.

The simplified parameters that were derived to represent the *p-y* curves for lateral vibration of single piles are presented in Tables 1 and 2. Several observations may be made from the tables: (1) the stiffness increases with confining pressure almost linearly in both plane stress and plane strain conditions; (2) the stiffness values are almost independent of the pile diameter (One should note that this is because it represents the region of soil that comprises the near-field zone, which is 40 times the diameter of the pile. The stiffness of the far-field element is a function of the diameter of the near-field zone and, thus, will reflect an increase in stiffness for the larger pile diameter.); (3) initial

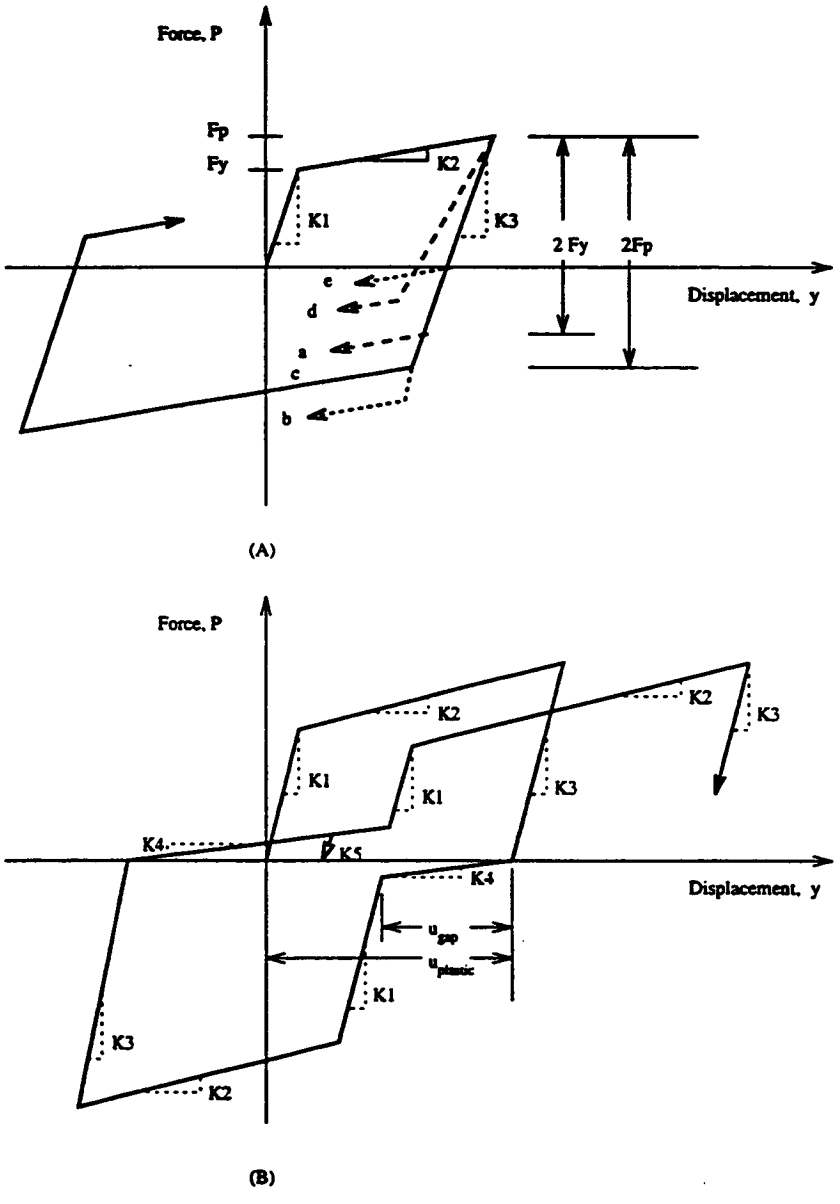

Figure 5. A linearized idealization of *p-y* curves.

Table 1. NEABS parameters for *p-y* curves for a single pile vibrating laterally for different confining pressures. [d = 18 in, K'_o = 0.50, f = 0.40, isotropic hardening, drained condition]

Vertical pressure, *psi*	Initial stiffness, lbs/in^2	Post-yield stiffness, lbs/in^2	Initial yield force *lbs/in*	First Gap stiffness, lbs/in^2	Hardening parameter, β	Gap parameter, γ
Plane-strain condition						
1	174.	46.	135.	5.	0.42	1.06
2.5	423.	71.	215.	7.	0.33	1.02
5	832.	117.	315.	11.	0.43	1.01
10	1692.	183.	529.	48.	0.62	1.19
20	2160.	291.	1034.	69.	0.60	1.13
40	2594.	617.	2062.	131.	0.49	1.03
80	3704.	1112.	4537.	314.	0.10	1.09
160	5474.	1865.	8711.	695.	0.41	1.02
Plane-stress condition						
1	157.	49.	143.	14.	0.33	0.54
2.5	389.	78.	218.	15.	0.58	0.71
5	868.	140.	354.	52.	0.15	0.73
10	1479.	195.	559.	100.	0.54	0.63

Table 2. NEABS parameters for *p-y* curves for a single pile vibrating laterally for different confining pressures. [d = 24 in, K'_o = 0.50, f = 0.40, isotropic hardening, drained condition]

Vertical pressure, *psi*	Initial stiffness, lbs/in^2	Post-yield stiffness, lbs/in^2	Initial yield force *lbs/in*	First Gap stiffness, lbs/in^2	Hardening parameter, β	Gap parameter, γ
Plane-strain condition						
1	179.	44.	175.	7.	0.55	1.07
2.5	429.	73.	278.	7.	0.35	1.03
5	857.	116.	419.	10.	0.43	1.03
10	1653.	192.	668.	19.	0.50	0.99
20	1921.	241.	1321.	76.	0.49	1.30
40	2762.	600.	2735.	159.	0.54	1.11
80	3931.	1384.	4484.	337.	0.43	1.05
160	5397.	1988.	12250.	702.	0.16	1.05
Plane-stress condition						
1	159.	53.	189.	24.	0.50	0.64
2.5	431.	70.	270.	28.	0.74	0.80
5	776.	100.	494.	37.	0.64	0.85
10	1913.	302.	581.	287.	0.58	0.40

stiffness is usually less in the plane stress case than in the plane strain case; (4) the yield force increases with confining pressure; (5) the yield forces are proportional to the diameters in both the plane stress and plane strain cases; (6) hardening occurs for all the *p-y* curves; and (7) the effect of the gap is more significant in the plane strain case than in the plane stress case.

Near-Field Damper

Due to the lack of viscosity data for the soil, the damping coefficient for the near-field element must be specified as a fraction of critical damping. Then, the damping constant is:

$$C = \frac{2\xi K}{\omega_{avg}}$$

where K is the initial or unloading/reloading stiffness of the near-field spring, ω_{avg} is the average loading frequency, and ξ is the material damping ratio.

The circular frequency for the actual earthquake loading may be estimated from the earthquake acceleration history of the free-field motion by counting the number of peaks or zero crossings, by Fourier analysis, or by considering the natural frequency of the structure involving predominantly foundation movement for inertial loading. The damping coefficient, ξ, is merely estimated as 0.01 to 0.10, based on engineering judgment and the magnitude of displacement at that particular level. The value of ξ can be obtained from the curves prepared by Hardin and Drnevich (1972) and Seed and Idriss (1969b). However, before using those curves, the average strain within the radius r_0 to r_1 should be known. The average value of strain should be taken as a function of the maximum displacement. Since the value of the displacement is unknown, the selection of the value of β becomes iterative. One may observe that the value of C is frequency dependent and, therefore, C must be defined for an estimated frequency. For higher frequencies of the loading, a specified value of C represents elevated values of ξ. However, high frequency loads are relatively unimportant for bridge design. Also, for high amplitudes of loading,

the hysteretic dissipation of energy is included with the nonlinear springs. Therefore, the use of proportional damping is considered to be a reasonable representation of the near-field damper.

Lumped Mass

Near-field masses are obtained from a lumped mass procedure. The model has two nodes: a pile node and an auxiliary node. The mass of the pile node consists of the mass of the pile itself along with the contribution of the mass from the near-field soil. The contribution of the mass from the soil is computed from the consistent mass matrix developed for the annular segment of soil with inner and outer radius r_0 and r_1, respectively, where r_0 is the radius of the pile and r_1 is the inner radius of the near-field zone. r_1 can be chosen arbitrarily such that all of the nonlinearity is contained within the near-field zone and the *p-y* curves should be consistent with this zone. In all cases, r_1 was taken as $40d$, where d is the pile diameter. The nodes are assumed to exist at the pile center and at the outer boundary, respectively. All points of the outer boundary of radius r_1 are assumed to have equal displacement and share the same degrees of freedom. The shape function in cylindrical coordinates is assumed to vary as a function of the nth power of r and it is not a function of the θ coordinate at all. The consistent mass matrix for the two nodes is

$$[M] = \left\{\frac{\left(\pi\rho r_0^2\right)(m-1)}{(n+1)(2n+1)}\right\}\begin{bmatrix} (2n+1)m+1 & \frac{n}{n+2}\{(2n+1)m+3\} \\ \frac{n}{n+2}\{(2n+1)m+3\} & m+(2n+1) \end{bmatrix}$$

where, $m = r_1/r_0$,

r_1 = radius of near-field zone,

r_0 = radius of rigid pile, and

n = power in the shape function.

In his analysis, Nogami assumed $n = 1$ arbitrarily. Using a lumping scheme, as described in the Technical Report (Cofer, et al. 1996), the contribution of the soil to the nodes as lumped mass is represented by the mass matrix,

$$[M]=\left\{\frac{(\pi\rho r_0^2)(m-1)}{2(n+1)(m+1)}\right\}\begin{bmatrix}\{(2n+1)m+1\} & 0\\ 0 & \{m+(2n+1)\}\end{bmatrix}$$

Having the mass contributions from the soil, the nodal mass at the pile node can be obtained by adding the nodal contribution from soil to the mass of the pile itself, as

$$m_p=\pi\rho_s r_0^2\left\{\frac{(m-1)\{m+(2n+1)\}}{2(n+1)(m+1)}+\frac{\rho_p}{\rho_s}\right\}s$$

where s = spacing of the node in the vertical direction.

The mass at the auxiliary node, m_a, can be obtained by adding two contributions, one from near-field soil and the other from far-field soil.

$$m_a = m_{11}+m_f$$

where, m_{11} = first diagonal element of [M], and

m_f = mass contribution from far-field soil.

The mass contribution, m_f, can be obtained from the equation

$$m_f = \pi\rho r_1^2\xi_m(\nu)$$

where $\xi_m(\nu)$ is a function of Poisson's ratio, given in the Technical Report (Cofer, et al. 1996).

Far-Field Elements

The far-field element consists of the far-field mass contribution, m_f, springs, K_1, K_2, and K_3, and dampers, C_1, C_2, and C_3. Those are shown in Figure 1. The far-field element has been adopted from Nogami, et al. (1992). The mass contribution from the far-field has been defined previously while the spring and damping constants are given as:

$$\begin{Bmatrix}K_1\\K_2\\K_3\end{Bmatrix}=G\xi_k(\nu)\begin{Bmatrix}3.518\\3.581\\5.519\end{Bmatrix}$$

$$\begin{Bmatrix}C_1\\C_2\\C_3\end{Bmatrix}=\frac{Gr\xi_k(\nu)}{V_s}\begin{Bmatrix}113.0973\\25.133\\9.362\end{Bmatrix}$$

where, G = Shear modulus of soil of the pertinent layer,

$\xi_k(\nu)$ and $\xi_m(\nu)$ = Function of Poisson's ratio ν, and

V_s = Shear wave velocity in soil.

The spring constants and damping constants are basically frequency dependent. However, the aforementioned values work well for the range of frequency, $0.02 < a_0 < 2.0$, where a_0 is the nondimensional frequency and it is defined as $a_0 = r_0\omega/V_s$, the commonly encountered frequency range for earthquake loading. The details are described by Nogami et al. (1992).

Axial Vibration of a Single Pile

This model is an extension of that proposed by Nogami and Konagai (1986, 1988). Analogous to the model for lateral vibration, it consists of two nodal masses at the pile node and an auxiliary node, a nonlinear near-field spring, a linear near-field damper, three linear far-field springs, and three far-field dampers, as shown in Figure 6.

The thin layer solution and Winkler hypothesis is again the basis of the model for axial vibration response. Moreover, it is assumed that during axial vibration of a single pile in semi-infinite soil, all points move only in the vertical direction. This simplifies the 3-D vibration problem to one of 2-D vibration, and allows the consideration of a thin layer solution, which is reasonable if the pile is long. Then, the thin layer is assumed to move vertically, and subsequent layers are assumed to move in the same way. Compatibility is thus maintained in an approximate manner, since each layer does not move equally. Resistances of different magnitudes develop at different depths depending on the shear modulus and pile displacement magnitudes.

For the assumption of no lateral displacement, only the shear deformation is included, rather than bending deformation of thin soil layers. This assumption applied to the skin resistance only. For the determination of the tip resistance, the pile tip is assumed to be on a nonlinear half-space with appropriate effective overburden pressure.

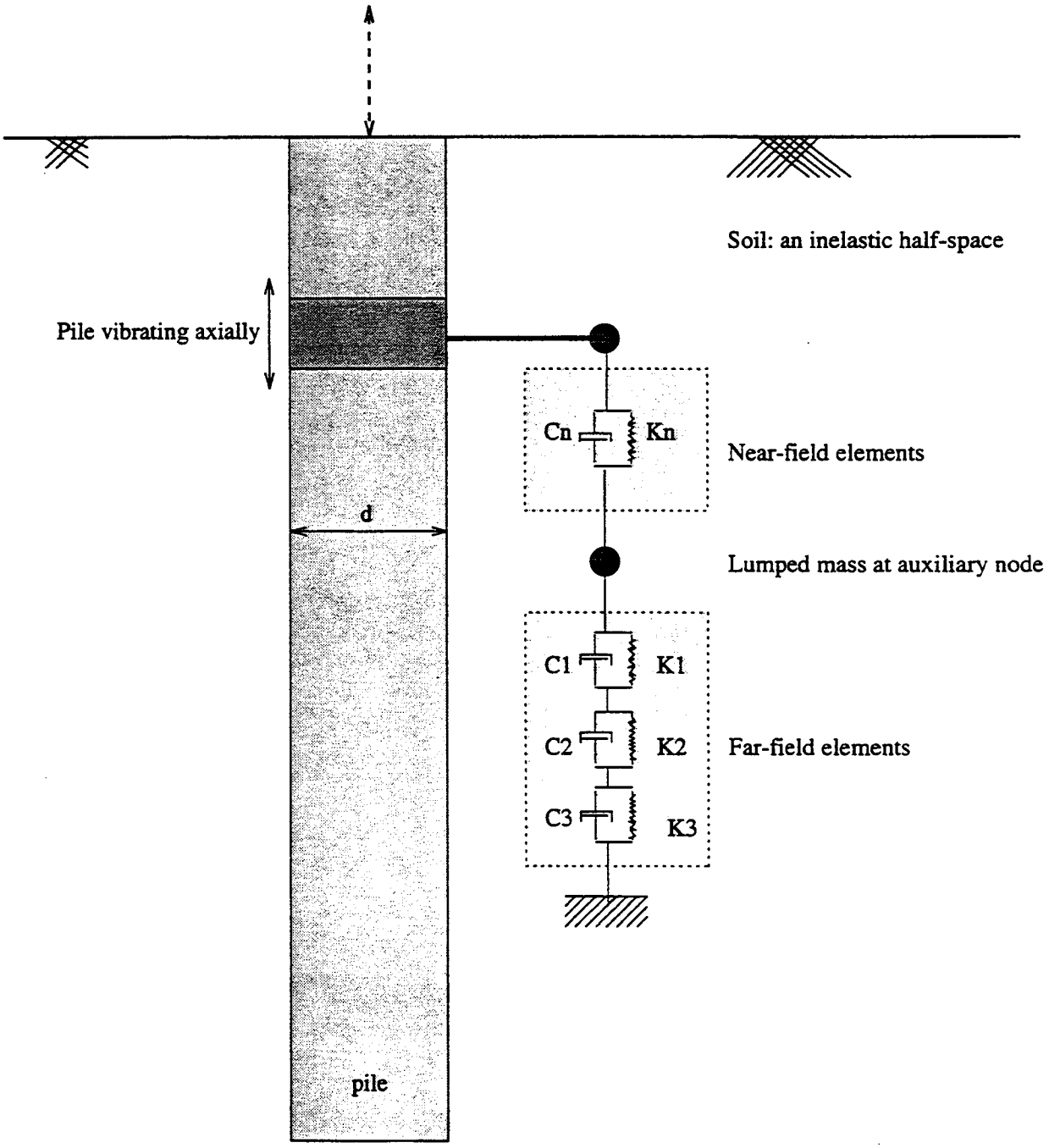

Figure 6. A model for axial vibration of single pile.

Near-Field Spring

To develop the nonlinear spring characteristics, a finite element model was developed for a thin layer elasto-plastic soil and rigid pile segment. Figure 7 shows a typical finite element model used to generate the nonlinear spring characteristics for axial vibration. Since a 3-D computer program without axisymmetric capability was used, it was necessary to model a sector of a thin circular segment. Soil within $8d$ of the pile was modeled with the geologic cap model. It was observed that soil displacement at a large distance (20 diameters) from the pile center was negligibly small and, therefore, an artificial, no displacement boundary was placed there. A pseudo-static load was applied along the pile axis to observe the resulting displacement. No sliding interface was assumed to exist between the pile and soil because initial observations showed that it induces instability. The initial K_0 state of stress was assumed as the initial condition. The overburden pressure was always maintained to ensure the confining effect.

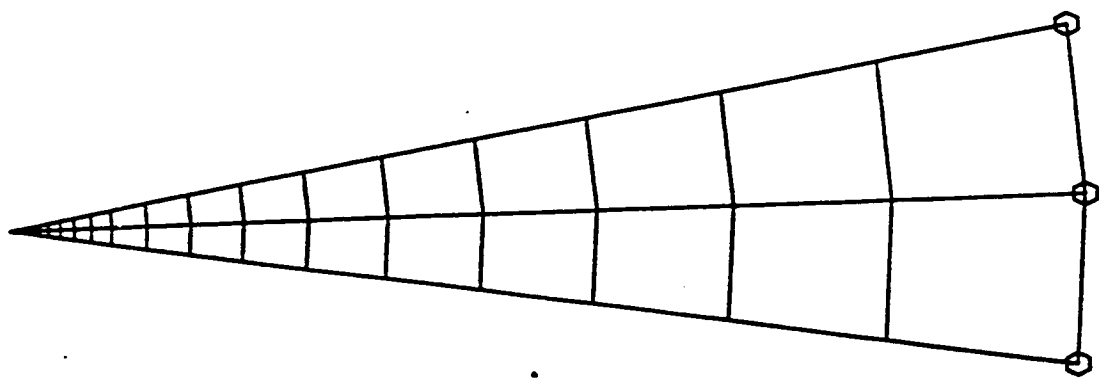

Figure 7. Finite element mesh used for the analysis of 2D soil-pile layer for axial vibration of single pile.

All nodes along the boundary were assumed to be fixed, and the rest of the nodes were allowed to move only vertically. The resulting force (per unit thickness) - displacement behavior, represented by *t-z* curves, were produced with eight different confining pressures for soil of the Snohomish river site, as given in the Technical Report (Cofer, et al. 1996). Most of the curves were obtained for a linear range of forces because, within the nonlinear range, the *t-z* response is non-hardening. Therefore, the response becomes unstable when it reaches or exceeds the yield force in a load controlled situation. Moreover, it was almost impossible to precisely estimate the yield force.

The bilinear parameters for the *t-z* curves are presented in Tables 3 and 4. The tables show that the initial stiffness increases with increasing confining pressure, although not linearly. Also, comparing the tables, one may observe that the stiffness of the near-field spring is almost independent of the pile diameter, which is unexpected. As with lateral vibration, this is caused by the fact that a larger soil region was included in the model for the larger pile diameter. However, the yield force is almost proportional to the pile diameters. Since the piles were analyzed in basically the linear range, the strength of the near-field springs must be estimated from the following equation:

$$t_{max} = (2\pi rt)\tau_{max}$$

The value of τ_{max} may be obtained elsewhere for specific soils. Finally, this spring behavior should be elastic-perfectly plastic, without hardening. Gap parameters are not necessary.

Near-Field Damper

Proportional damping can be used in the same way as for lateral vibration. The damping ratio is for the material damping alone. The explicit value of C can be computed as:

$$C = 2\xi K_i/\omega$$

where, K_i = initial or unloading/reloading stiffness,
ω = average loading frequency , and
ξ = effective material damping ratio.

Table 3. NEABS parameters for *t-z* curves for single pile vibrating axially for different confining pressures. [d = 18 in., K'_o = 0.50, isotropic hardening, drained condition]

Vertical pressure, *psi*	Initial stiffness, lbs/in^2	Post-yield stiffness, lbs/in^2	Initial yield force *lbs/in*	Hardening parameter, β
1	155.			
2.5	285.	3.	279.	0.000
5	810.	21.	352.	0.000
10	1020.	0.	552.	0.000
20	1246.	0.	955.	0.000
40	2093.			
80	2621.			
160	3774.			

Table 4. NEABS parameters for *t-z* curves for single pile vibrating axially for different confining pressures. [d = 24 in., K'_o = 0.50, isotropic hardening, drained condition]

Vertical pressure, *psi*	Initial stiffness, lbs/in^2	Post-yield stiffness, lbs/in^2	Initial yield force *lbs/in*	Hardening parameter, β
1	153.			
2.5	398.	45.	357.	0.000
5	807.			
10	1618.			
20	1934.			
40	2092.			
80	2625.			
160	3768.			

Lumped Mass

For a thin layer of soil with a pile segment, only two degrees of freedom are needed to model the vibration: the pile node and an auxiliary node. During the axial vibration, the whole layer of the soil vibrates along with the pile. Therefore, some inertial resistance comes from the soil, and for the sake of modeling, a certain part of the soil layer should be assumed to contribute to the inertial resistance of the pile. For a point in a soil layer at a large distance away from the pile, the amplitude decays and becomes less important. A shape function may, therefore, be applied to compute the soil contribution. The shape function assumed here is the approximate displacement shape of the same layer of elastic soil with a rigid pile segment. The resulting consistent mass matrix is:

$$[M] = \left\{\frac{2\pi\rho_s t r_1^2}{[\ln(r_1 / r_0)]^2}\right\}\begin{bmatrix} f_{11}(m) & f_{12}(m) \\ f_{21}(m) & f_{22}(m) \end{bmatrix}$$

where

$$f_{11}(m) = 1/4 - \{1 + 2(\ln m) + 2(\ln m)^2/m^2\},$$

$$f_{12}(m) = (3/4)(m^2 - 1)(\ln m)(1/m^2) - f_{11}(m),$$

$$f_{22}(m) = f_{11}(m) + (1/2)(1 - 1/m^2)\{1 - 3/(\ln m)\},$$

$$m = r_1/r_0.$$

After lumping, the following consistent mass marix was obtained:

$$[M'] = \{\pi(r_1^2 - r_0^2)\rho_s t\}\begin{bmatrix} f_{11}'(m) & 0 \\ 0 & f_{22}'(m) \end{bmatrix}$$

where

$$f_{11}'(m) = \frac{f_{11}(m)}{f_{11}(m) + f_{22}(m)}, \text{ and}$$

$$f_{22}'(m) = \frac{f_{22}(m)}{f_{11}(m) + f_{22}(m)}.$$

The contribution of mass from the near-field soil to the pile, m_p, and to the auxiliary node, m_a, are:

$m_p = \pi r_0^2 \rho_s t(m^2 - 1) f_{11}'(m)$, and

$m_a = \pi r_0^2 \rho_s t(m^2 - 1) f_{22}'(m)$, respectively.

The above expressions will only work well for low frequency vibrations. The shape function that was assumed will not represent the actual displacement behavior during high frequency vibration, for which the mass contribution is reduced due to both positive and negative contributions of the soil from wave effects. The effect of soil mass would be further reduced for nonlinear soil because most of the effects are local during nonlinear vibration.

MODELING OF PILE GROUPS

For the vibration of two-pile groups, in addition to the near-field and far-field elements considered for a single pile, it is necessary to consider interface springs between piles. In general, there are three near-field nonlinear springs required for each pile node, three nonlinear interaction springs required for each pile-soil-pile connection, and three sets of far-field elements required for each external pile for modeling 3-D vibration of a general pile group.

For the sake of modeling, it is expected that three interaction springs (i.e., direct-lateral, shear-lateral, and axial springs) between two isolated piles for general vibration will be required to represent the interaction between neighboring piles. So, in a large group, each pile will be connected with neighboring piles by direct-lateral, shear-lateral, and axial interaction springs. For even closely spaced pile groups, say with $2d$ clear spacing (i.e., $3d$ center spacing), the far neighbors will have a $5d$ clear spacing (i.e., $6d$ center spacing). For this spacing, interaction can be neglected. For this interaction model, it is assumed that the consideration of interaction between neighboring piles only is sufficient for engineering accuracy. For the interaction of more than two-pile groups, the interaction spring behavior may be obtained from that of two piles. The Winkler hypothesis was again the basis of this approximate model for the pile-soil-pile interaction for axial and lateral vibration for earthquake loading.

Characteristics of Springs in Two-Pile Groups

There are three basic types of springs in pile group models. These include nonlinear near-field springs, nonlinear interacting springs, and linear far-field springs. Nonlinear near-field springs are required for those connecting piles with surrounding soil, and nonlinear interacting springs are required for those connecting the piles themselves.

The nonlinear spring elements for the modeling of a two-pile group with near-field and interaction springs are shown in Figure 8 for uniaxial lateral vibration and in Figure 9 for biaxial lateral vibration. From Figure 8, it is observed that one load case is necessary to determine the force/displacement behavior for the three near-field springs required for direct lateral vibration. The load case, in which one segment is moved and the other is kept fixed, is required to get the characteristics of the interaction spring, *K2*, and the near-field spring, *K1*. Then, it may be considered that the behavior of *K3* and *K1* are the same both in compression and tension.

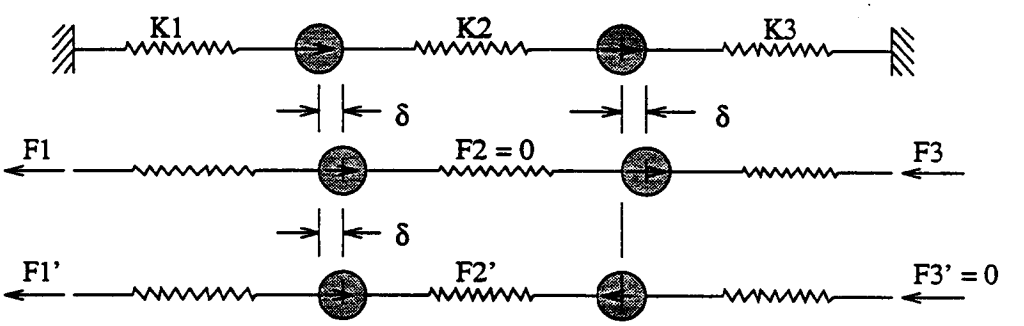

Figure 8. Model for direct-lateral vibration of a two-pile group moving laterally along the line which passes through the piles.

For two-pile groups with vibration in both direct lateral and shear lateral directions, two types of additional springs are required. One is an interaction shear spring and the other is a near-field spring for connecting pile segments with the surrounding soil. An additional load case is required to establish the behavior of these springs, denoted as *K4* and *K6* in Figure 9.

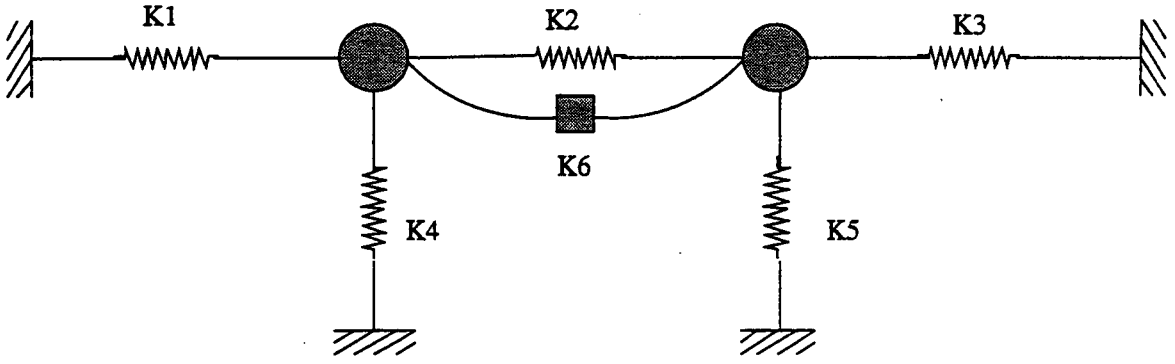

(A)

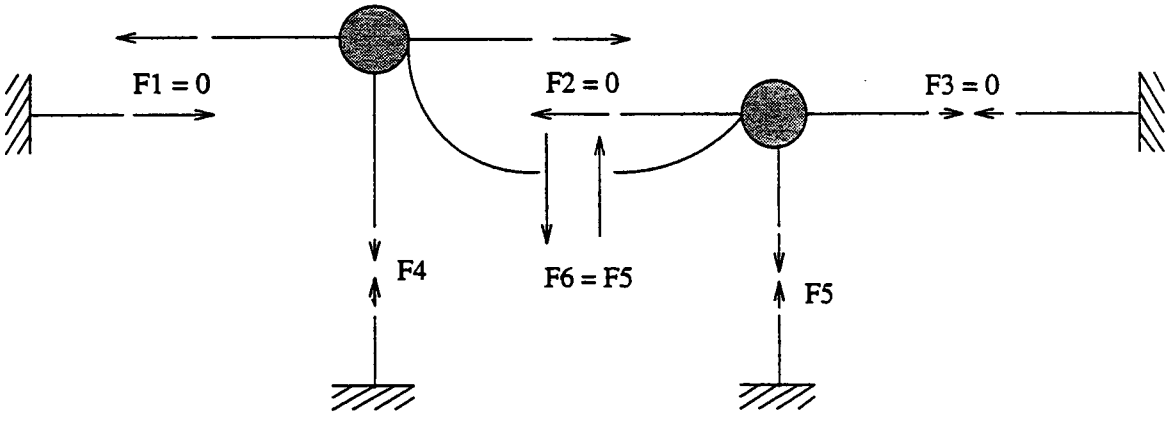

(B)

Figure 9. A more general model for vibration of a two-pile group for direct-lateral and shear-lateral vibration.

As expected, the behavior of spring *K1* in tension is the same as that of *K3* in compression. However, they should have different yield forces in tension and compression. On the other hand, springs *K2*, *K4*, *K5*, and *K6* are expected to behave in the same manner in both tension and compression. Also, spring *K6* should behave similarly in positive and negative shear. Moreover, as the spacing between two piles, *s*, increases, the stiffness of the interaction springs, *K2* and *K6*, are expected to diminish, and *K1*, *K3*, *K4*, and *K5* should tend to those for a single pile. Then, *K1*, *K3*, and *K4* should have the same yield strengths.

Direct Lateral Springs

The characteristics of the interaction springs for different confining pressures and for drained conditions were determined for soil taken from the Snohomish river site. For the determination of the direct interaction spring constants for lateral vibration, plane strain conditions were assumed for all depths represented by 1, 2.5, 5, 10, 20, 40, 80, and 160 psi (6.9, 17.3, 34.5, 68.9, 137.8, 275.6, 551.2, and 1102.4 kPa) vertical stress. Plane stress was assumed for confining pressures of 6.9 and 34.5 kPa (1 and 5 psi). Due attention was given to the initial K_0-stress condition and constitutive modeling of elastic and elasto-plastic soil. The displacement at a distance of $20d$ from the pile was assumed to be zero, and a zone of radius $4d$ was assumed to be the zone of nonlinearity. Within the nonlinear zone, soil was modeled using the geologic cap model while, beyond the nonlinear zone, it was modeled with elastic assumptions. At the boundary of these zones, the observed strains were small, implying that the elastic constitutive model of soil is applicable in the far-field. Moreover, the pile-soil interface was modeled with sliding interface elements with a coefficient of friction of 0.4. The finite element model is shown in Figure 10. The condition of symmetry was used to conserve computer resources.

A pseudo-static load was applied on one rigid segment of the pile either toward the other pile or in the reverse direction, varying sinusoidally with a very low frequency and low rate of loading, keeping the other pile fixed. The resulting displacement in the first pile, and active or reactive force on both piles, were observed and analyzed to

establish the *p-y* behavior of the two-pile group. The resulting *p-y* behavior of the interaction springs and the near-field springs along with the gap parameters are given in the Technical Report (Cofer, et al. 1996).

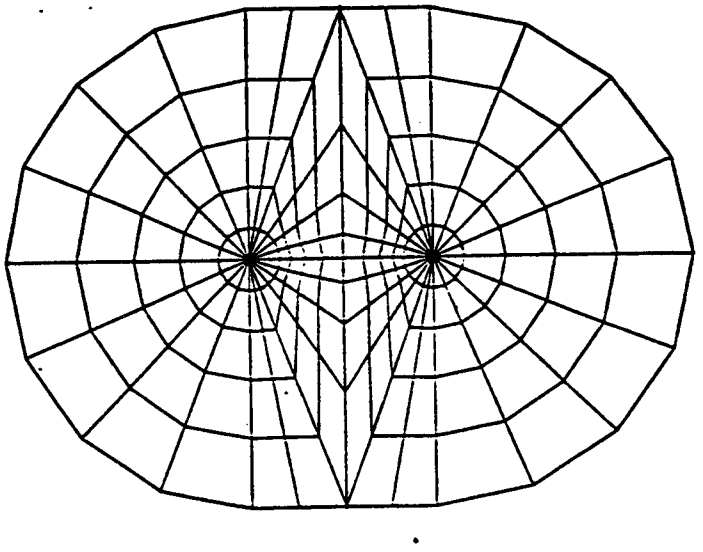

Figure 10. Finite element mesh used for the analysis of 2D pile-soil-pile layer.

From the results, one may observe that the stiffness of the interaction springs decreases with increasing spacing, while the stiffness of the near-field springs increases with increasing spacing. All of the springs displayed hardening and the gap effect was shown to be very significant.

Shear Lateral Springs

For the computation of shear lateral interaction spring behavior, the same mesh, as shown in Figure 10, was used without the assumption of symmetry. The same procedure as that used for the direct interaction springs was applied, except that the motion was prescribed in the transverse direction. The resulting *p-y* behavior of the interaction springs and the near-field springs along with the gap parameters are given in the Technical Report (Cofer, et al. 1996).

All of the observations for the interaction springs for direct lateral vibration regarding the effects of spacing apply equally well to those for shear lateral vibration except that the stiffness is much less. Thus, as one may expect, the direct lateral interaction is much more prominent than shear lateral interaction in dynamic group behavior.

Axial Springs

As with modeling lateral vibration, interaction springs are included for the axial vibration of pile groups. These interaction springs resist the shear of relative vertical displacements and they are assumed to behave in the same way for both directions of loading. The near-field and far-field elements, with their masses and dampers, are still applied to connect the pile to the soil. For the determination of the spring characteristics, it is again assumed that no point in the soil moves laterally during axial vibration of piles in pile groups.

For the determination of axial interaction and near-field springs, two piles were again modeled as a thin layer, as shown in Figure 10. Only vertical displacement was allowed and perturbation was given to one pile while the resulting displacement and reactive force on the other pile were observed and analyzed to obtain the interaction characteristics. The resulting *t-z* behavior of the interaction springs and the near-field springs, along with gap parameters, are given in the Technical Report (Cofer, et al. 1996).

The effect of spacing was again similar to that of the lateral interaction springs. For the axial interaction springs, however, the hardening with displacement was observed to be insignificant. Also, during the analysis, it was assumed that the interface is perfect and that no gap is formed. The results show that slippage occurs, causing perfectly plastic *t-z* behavior.

Dampers

As with the near-field elements, dampers for the interaction elements are based on Rayleigh's proportional damping for the dominant loading frequency:

$$C = \frac{2\xi K}{\omega}$$

where, again, K is the initial or unloading/reloading stiffness of the interaction spring, ω is the average loading frequency, and ξ is the material damping ratio.

Masses

The nodes corresponding to pile segments can have a mass from the pile itself and a contribution from the soil. The concept of tributary area may be used for the determination of lumped masses. The contribution from the soil to an interior pile segment may be considered to come from the hatched region, as shown in Figure 11.

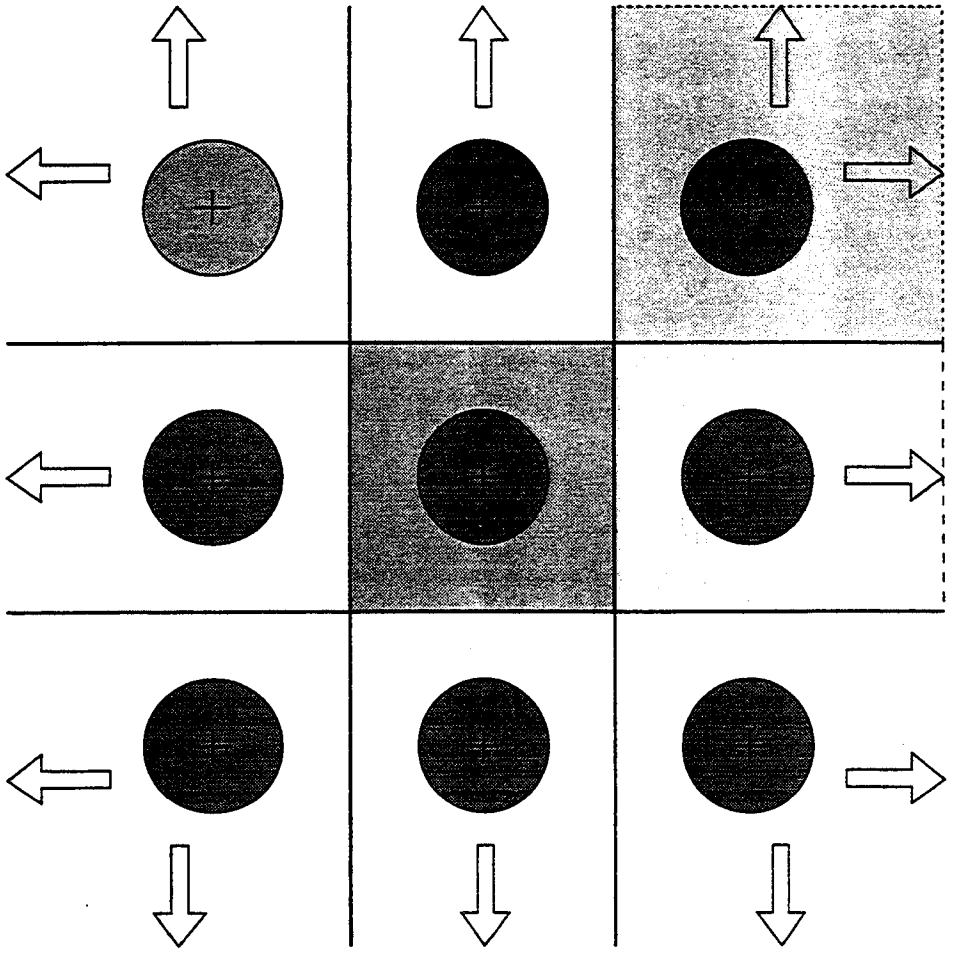

Figure 11. Concept of tributary area employed to find approximate mass contributions from soil to the piles in a pile group.

Then, for the piles at the center,

$$m_p = [\rho_p \pi r_0^2 + \rho_s (S_1 S_2 - \pi r_0^2)]s$$

where r_p and r_s are mass density of the pile and soil, respectively; r_0 is the radius of the pile; S_1 and S_2 denote pile spacing in two orthogonal directions; and s is the spacing of the node in the vertical direction.

For piles on the sides and at the corners of the group, the mass contibution of the soil also comes from a large distance. This contribution to the mass can be estimated by considering tributary area and an approximate shape function. The consistent mass matrices can then be developed. A lumping scheme may then be followed to get a diagonal mass matrix, which is then used to identify the contribution of soil to the lumped nodal masses. For piles on a side,

$$m_p = (\pi r_0^2 \rho_s)\left\{\frac{2LS_1}{\pi r_0^2}\frac{n^2}{(2n^2+n+1)} + \frac{S_1 S_2}{2\pi r_0^2} + \left(\frac{\rho_p}{\rho_s} - 1\right)\right\}s$$

where L is the distance between the pile center and the near-field boundary and n is the power in the shape function.

For piles at a corner,

$$m_p = \left[\frac{S_1 S_2 \rho_s}{4} + \rho_s\left(\frac{n^2}{2n^2+n+1}\right)(L_1 S_1 + L_2 S_2 + 2L_1 L_2) + \pi r_0^2 \rho_s\left(\frac{\rho_p}{\rho_s} - 1\right)\right]s$$

where L_1 and L_2 denote distance from the center of the pile to the boundary of the near-field in two orthogonal directions.

Far-Field Elements

In the estimation of the far-field elements, it may be assumed that the waves produced by the inner piles of the group are reflected by the piles around them. Thus, the radiation energy dissipated from the inner piles comes back into the system. However, it may be assumed that the waves generated by the surrounding piles either at the sides or at the corners of the group do not come back.

Therefore, modeling of the far-field for a pile group can be done by connecting far-field elements to the surrounding piles with the near-field elements through auxiliary nodes. Furthermore, for the sake of modeling, it may be assumed that piles in the group do not interact with each other in the far-field. Then, the far-field elements connecting a pile in a pile group may be assumed to be those for a single pile. Alternatively, the far-field spring stiffnesses, damping coefficients, and the lumped masses for a single pile which is equivalent to the pile group can be distributed along the external pile using a reasonable ad hoc procedure. In this case, a reasonable equivalent radius of the pile group would be required.

PILE CAP BEHAVIOR

In almost no cases are solitary piles used. Piles come in groups and they are usually connected at the top with a relatively rigid pile cap. If the cap is connected to the soil and embedded in it, it will produce lateral resistance. The lateral resistance has two sources: bearing and shearing along the vertical surface and shearing along the bottom surface.

Near the soil surface, the confining pressure is small. The soil is normally soft and the vertical surfaces contribute little to the pile group resistance compared to that of the piles. To model this resistance, *p-y* curves were developed for circular and rectangular pile caps of different dimensions in the same way as was done for single piles, and they are useful for lateral vibration analysis. During the analysis, rigid cap behavior, elasto-plastic and elastic behavior of the soil in the near- and far-field zones, respectively, sliding interfaces, and plane stress conditions were considered. Displacement of the soil at a distance of $20d$ or $20a$ (d, a = dimensions of circular and square caps, respectively) was considered to be negligible by providing an artificial, no displacement boundary. The resulting *p-y* curve was generated for four different sizes of square and four different sizes of circular pile caps for the soil of the Snohomish river site. Specific *p-y* curves and NEABS parameters are given in the Technical Report (Cofer et al. 1996).

PILE TIP BEHAVIOR

The vertical force-displacement relation for axial response, T_t-Z_t, of the pile tip is much more important for end-bearing piles than friction piles. Pile tip vertical response is also important for lateral response of pile groups. The lateral response for the pile tip, P_t-Y_t, is important for determining the lateral response of end-bearing piles and pile groups. For the determination of the lateral response of the pile tip, an actual 3-D analysis is required. However, the lateral force-displacement behavior for the perfectly elastic condition is available in the literature (Wolf 1988) and it is deemed to be acceptable for engineering applications.

Alternatively, the use of the pile tip response may be avoided by considering a soil column as part of the pile with soil material properties. The near-field and the far-field elements can be added to this extended soil column. Nogami and Konagai (1986, 1987) adopted this concept in their work.

The interaction between pile tips may also be considered. However, the designer may adopt the elastic interaction factors. In that case, one should keep in mind that interaction effects reduce with increasing plasticity, and elastic interaction factors are the upper limits of those factors.

FINDINGS

LATERAL RESPONSE OF A SINGLE PILE

The proposed model has been evaluated by simulating a dynamic pile test. Its response is compared to that obtained from a three dimensional finite element model of pile-soil interaction with sliding interfaces for lateral loading. A single 24-inch (0.632 m) pile was modeled, as shown in Figures 12 and 13. The length of the pile was 22.5d. In the finite element model, the diameter and length of the soil domain was 20d and 36d, respectively. The soil nonlinearity, pile-soil slippage, gap formation, and initial geostatic stress were considered. The damping was assumed to come from geometric damping and

hysteretic damping. The infinite soil domain was simulated using a finite soil domain with non-reflecting boundaries. The condition of symmetry was utilized. The pile was assumed to be linearly elastic.

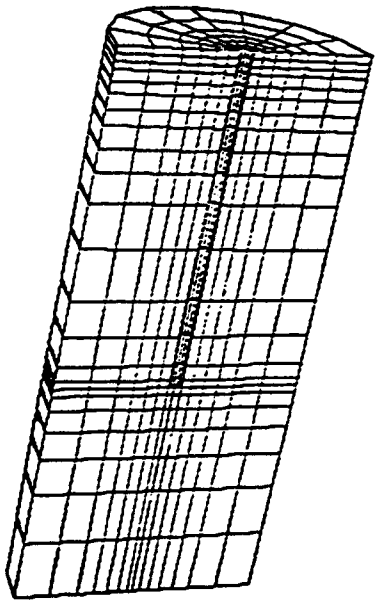

Figure 12. The FEM model used for the analysis of lateral vibration of a single pile.

The discrete model was constructed of beam-column elements with lumped masses, nonlinear springs, and linear dampers to represent near-field and far-field behavior. For the nonlinear near-field springs, the previously described *p-y* curves were used. They were scaled by the thickness of the layer to get the proper resistance. Consistent mass and proportional damping were also considered in the near-field. Similarly, the springs, masses, and dampers of the far-field elements were applied in accordance with the recommendations of Nogami, et al. (1992).

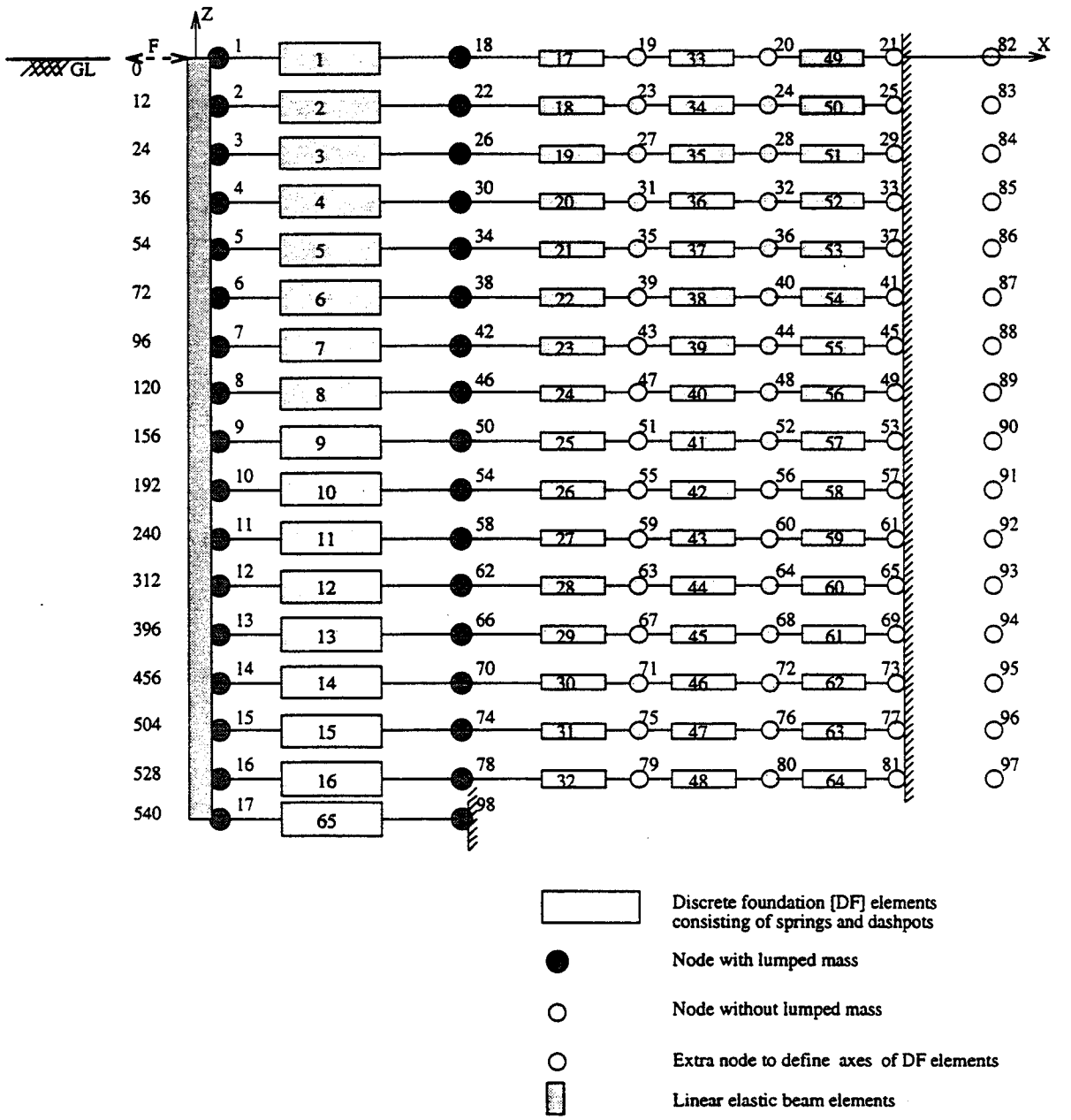

Figure 13. The lumped models used for the analysis of lateral vibration of a single pile.

A harmonic forced transient response was modeled. The forcing function was a half-sine wave with an amplitude of 150 kips, as shown in Figure 14. The duration of loading was one second, and the analysis was performed for two seconds. The peak load was attained at time $t = 0.5$ seconds. The pile head displacement histories are plotted in Figure 15 for two cases of pile end conditions and two values of near-field viscous damping.

One may observe that the head displacement results obtained from the finite element model compare well with those of the discrete model with high damping in the near-field element. Although no Rayleigh damping was assumed in the finite element model, the results show high damping in the response. This is most likely caused by the fact that energy is dissipated at a high rate through the non-reflecting boundary. Another possible cause is the artificial damping that is included in DYNA3D to suppress zero energy modes in the 8-node solid elements used to represent the soil. Because of the large computational requirements of the finite element model, however, only one analysis was feasible and parametric studies were not performed.

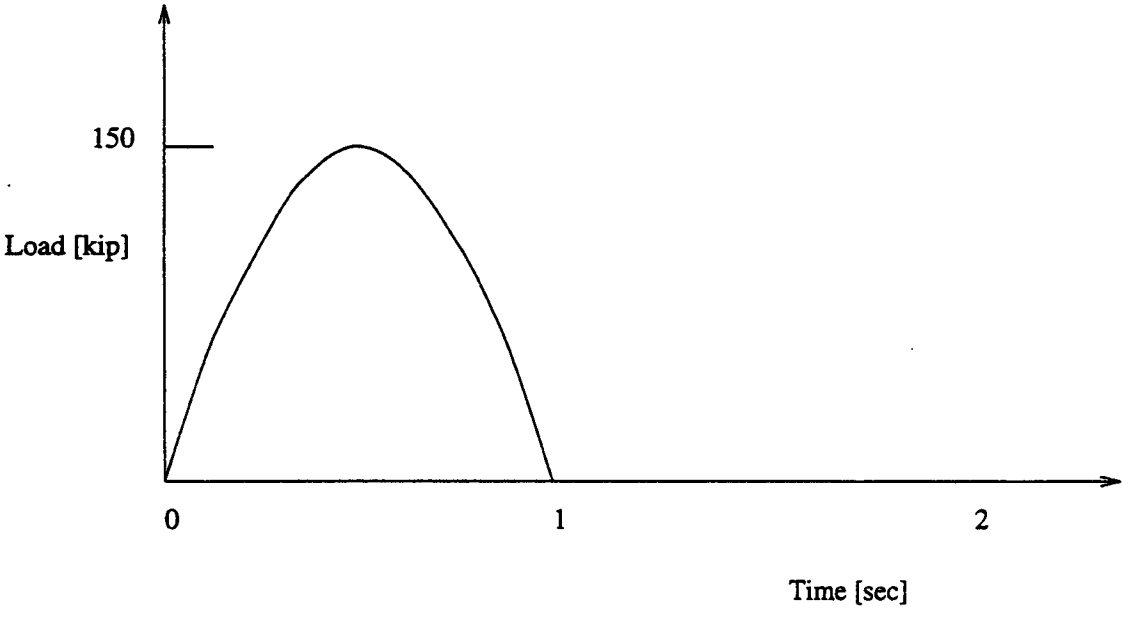

Figure 14. The load history used to analyze the lateral vibration of the single pile.

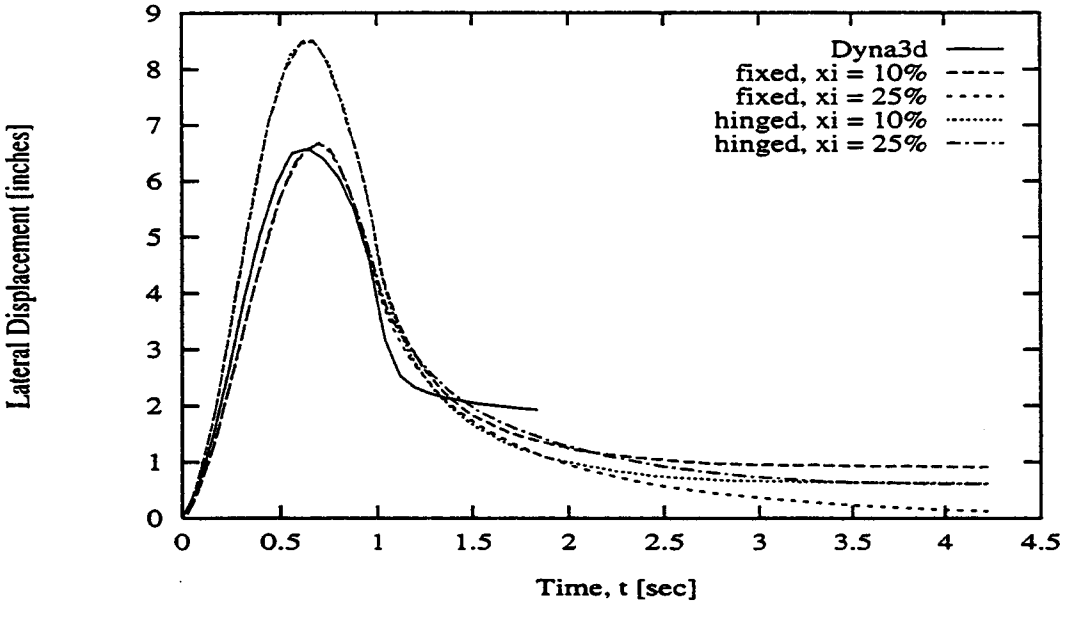

Figure 15. The pile head displacement histories obtained from the discrete model.

CONCLUSIONS

The main objective for this research was to develop a simplified lumped-parameter model of pile foundations for bridges for the time domain analysis of the response due to earthquake excitation. A procedure was developed to define lumped parameters for nonlinear near-field springs on the basis of two-dimensional finite element analysis and an appropriate soil model. The properties of the soil model were evaluated from tests on a typical soil from Washington State. The near-field mass and damping properties were obtained in a logical way, while the elements that model the far-field were obtained from the literature. For pile groups, interaction springs and dampers were similarly developed.

In order to evaluate the performance of the discrete model of a single pile, a comparison was made with the response from an equivalent three-dimensional finite element analysis of the same pile when subjected to an impulse loading. Although neither model is "exact", the discrete model was shown to provide a response of the same order as that of the finite element model. The discrete model has thus been demonstrated to be a reasonable engineering alternative to complex finite element models.

IMPLEMENTATION

The proposed model can be implemented in any time domain finite element computer program which can handle discrete elements such as linear and nonlinear springs, linear dashpots, lumped mass, and a beam element with or without geometric stiffness. However, the nonlinear springs should have special features such as gap stiffness in addition to the usual nonlinear stiffness behavior. The program, NEABS, which has been modified (McGuire, et al. 1994) as a companion phase of the present research, has all of the capabilities required for the proposed model. Therefore, this version of NEABS is recommended.

Although the Winkler model of single piles and pile groups has been shown to provide reasonable results for dynamic analyses, the sheer number of beam, spring, mass,

and dashpot elements that is required for each pile makes this model cumbersome for large bridge models. However, simplified foundation modeling can be performed in one of two ways.

For the first approach, as mentioned by Elassaly, et al (1995), the Winkler model of the foundation could be analyzed with the stiffness and mass properties of the bridge superstructure included in only a very simplified way. The seismic acceleration record could be applied along the length of the pile, and the resulting acceleration values at the top of the pile could then be used as input to a more detailed bridge superstructure model.

With the second approach, the pile or foundation model can be treated in essentially the same way as in an experimental test. A harmonic excitation can be applied to the top of the foundation model and impedances can be calculated for use in a linear modal analysis. It has also been shown (McGuire et al. 1994) that reasonable results for the nonlinear response of a bridge bent in the time domain were obtained by applying the spring, mass, and damper values obtained from the impedance properties of a spread footing foundation which were evaluated for the fundamental natural frequency of the structure.

A procedure for evaluating the equivalent single-degree-of-freedom properties of a system subjected to harmonic loading may be found in texts on structural dynamics (e.g., Clough and Penzien 1993). Here, two analyses must be performed with harmonic load at the top of the foundation for two separate frequencies, ω_1 and ω_2, and a force amplitude of p_o. From the solution, the response amplitude values, ρ_1 and ρ_2, and the phase angles, θ_1 and θ_2, may be determined. Then, the following equation holds for each solution:

$$k - \varpi^2 m = \frac{p_o \cos\theta}{\rho}$$

Thus, the two equations may be used to solve for the two unknown parameters, k and m. The damping, c, is frequency dependent and its value for each excitation may be computed by the following:

$$c = \frac{p_o \sin\theta}{\varpi \rho}$$

As an example, the pile model that was used for calibration was evaluated to determine an equivalent spring-mass-damper system. Four solutions were generated for excitation frequencies of 1 hz and 2 hz and force amplitudes of 50 kips (222.4 kN) and 100 kips (444.8 kN). The two values of force amplitude were chosen to consider the response for a case in which all aspects remain linear versus one in which the foundation springs behave nonlinearly. Figures 16 - 19 show plots of the response of the top of the pile for all analyses and the results are given in Table 5.

Table 5. Pile response data and equivalent properties for the single pile model

Loading Frequency (hz)	Force Amplitude (kips)	Response Amplitude (inches)	Phase Angle (deg.)	k (kips/in)	m (lb-sec^2/in)	c (lb-sec/in)
1	50	1.99	7.56	25.81	22.02	602.4
2	50	2.12	18.72	25.81	22.02	526.9
1	100	6.55	28.44	14.54	28.14	524.4
2	100	8.29	33.12	14.54	28.14	1158

As a point of comparison, the static stiffness of the pile in the elastic region was computed to have a value of 24.30 kips/in, which compares within engineering accuracy to the dynamic stiffness obtained from the lower force amplitude. In comparison, the stiffness from the higher amplitude load is significantly reduced, reflecting the increased flexibility in the soil springs due to yielding. The main benefit of using this method, as compared to simply computing a reduced stiffness value for the foundation in the nonlinear region, is that mass and damping values may also be obtained in a rational way.

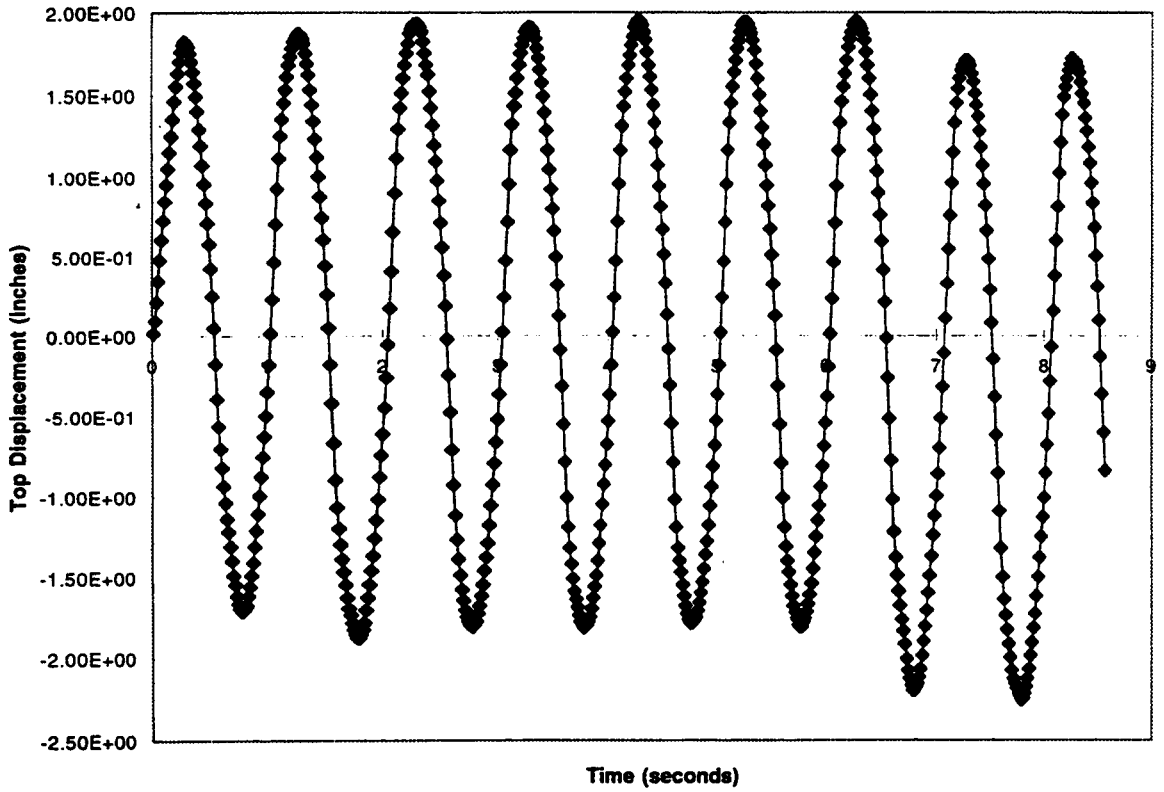

Figure 16. Pile Head Response, 50 Kip Lateral Load at 1 hz

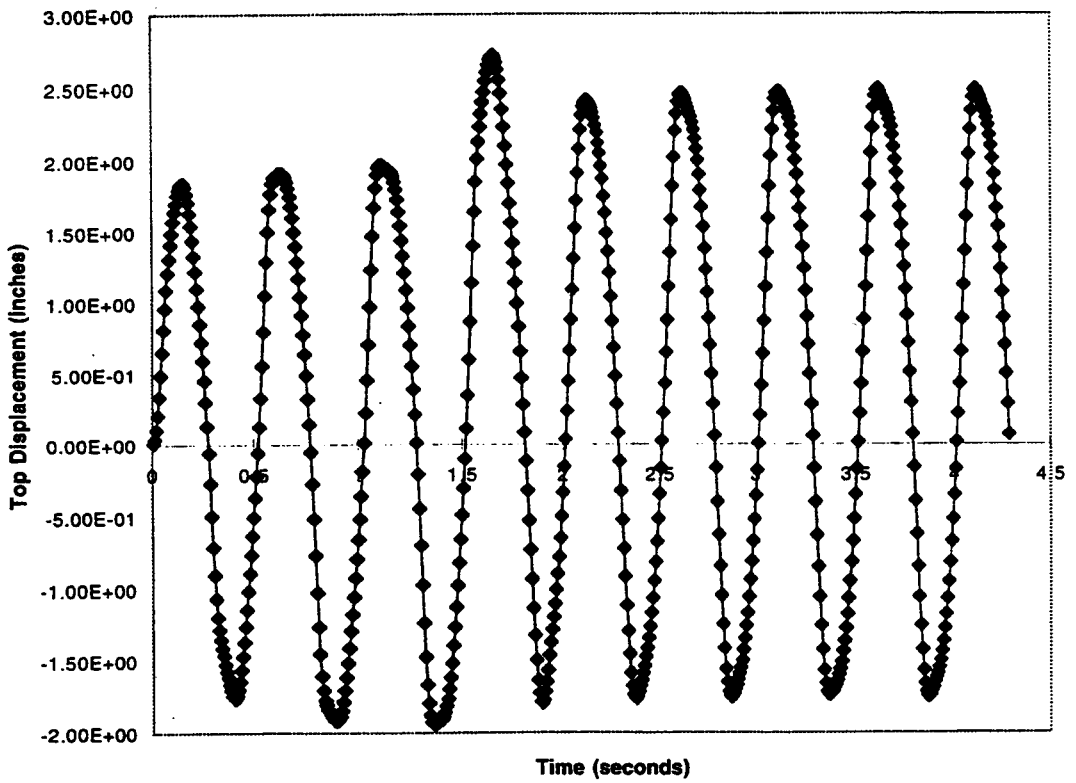

Figure 17. Pile Head Response, 50 Kip Lateral Load at 2 hz

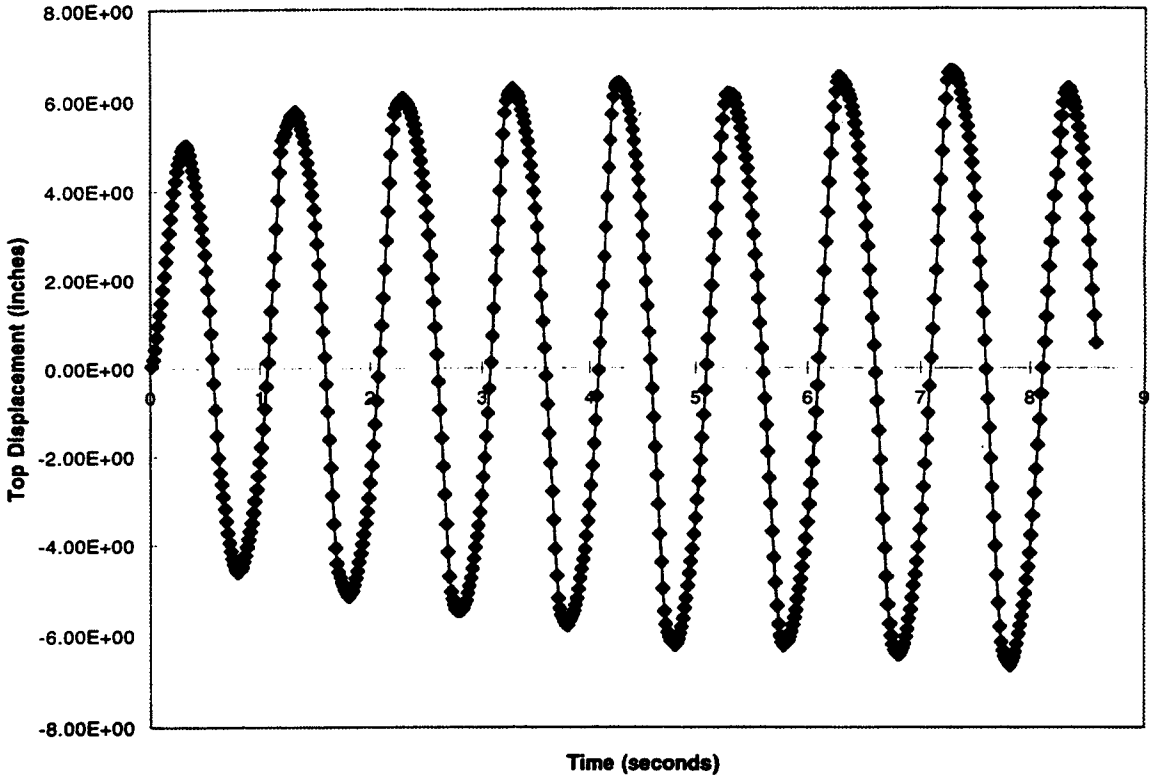

Figure 18. Pile Head Response, 100 Kip Lateral Load at 1 hz

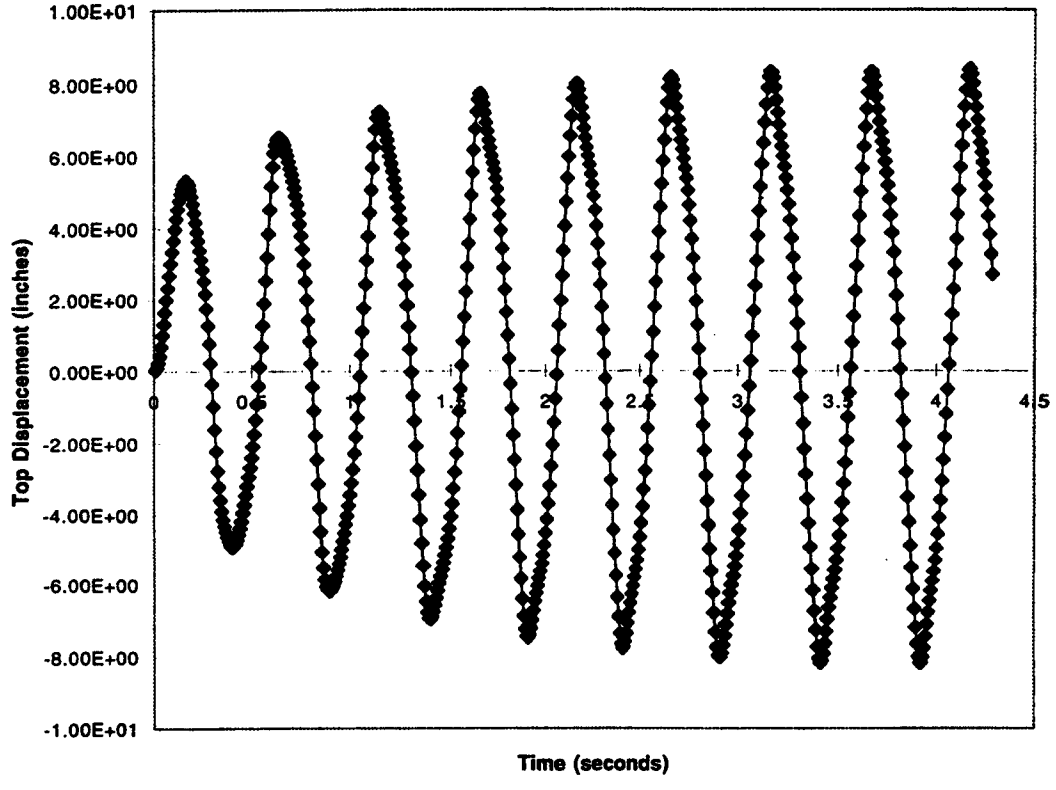

Figure 19. Pile Head Response, 100 Kip Lateral Load at 2 hz

REFERENCES

Brown, D. A. And Shie, C. F. (1990). "Three Dimensional Finite Element Model of Laterally Loaded Piles," *Computers and Geotechnics*, **10**, 59-79.

Cofer, W. F., McLean, D. I., and McGuire, J. W., (1994). "Analytical Modeling of Foundations for Seismic Analysis of Bridges," Washington State Transportation Center, Final Technical Report No. WA-RD 328.2.

Cofer, W. F. and Modak, S. (1996). "Determination of Rheological Parameters of Pile Foundations for Bridges for Earthquake Analysis," Olympia, Washington: Washington State Department of Transportation, Draft Technical Report No. WA-RD 406.1.

Clough, R. W. and Penzien, J., (1993). *Dynamics of Structures*, 2nd Edition, McGraw-Hill, Inc., New York.

Elassaly, M., Ghali, A., and Elbadry, M. M., (1995). "Influence of Soil Conditions on the Behaviour of Two Cable-Stayed Bridges," *Canadian Journal of Civil Engineering*, **22**, 1021-1040.

El Sharnouby, B. and Novak, M. (1985). "Static and Low-Frequency Response of Pile Groups," *Canadian Geotechnical Journal*, **22**, 79-94.

Hardin, B. O. and Drnevich, V. P. (1972). "Shear Modulus and damping of soils: Measurement and parameter effects," *Journal of the Soil Mechanics and Foundation Division, ASCE.* **98**(SM6), 603-624.

Jardine, R. J., Potts, D. M., Fourie, A. B., and Burland, J. B. (1986). "Studies of the Influence of Non-Linear Stress-Strain Characteristics in Soil-Structure Interaction," *Geotechnique*, **36**(3), 377-396.

Leung, C. F. and Chow, Y. K. (1987). "Response of Pile Groups Subjected to Lateral Loads," *International Journal for Numerical Methods in Geomechanics*, **11**, 307-314.

Makris, N. and Gazetas, G. (1992). "Dynamic Pile-Soil-Pile Interaction. Part II: Lateral and Seismic Response," *Earthquake Engineering and Structural Dynamics*, **21**(2), 145-162.

Mamoon, S. M. and Banerjee, P. K. (1990). Response of Piles and Pile Groups to Travelling SH-Waves," *Earthquake Engineering and Structural Dynamics*, **19**, 597-610.

McGuire, J. W., Cofer, W. F., Marsh, M. L. and McLean, D. I. (1994). "Analytical modeling of spread footing foundations for seismic analysis of bridges," *Transportation Research Record*, **1447**, 80-92.

Muqtadir, A. and Desai, C. S. (1986). "Three-Dimensional Analysis of a Pile-Group Foundation," *International Journal for Numerical and Analytical Methods in Geomechanics*, **10**, 41-58.

Nogami, T. (1985), "Flexural Responses of Grouped Piles Under Dynamic Loading," *Earthquake Engineering and Structural Dynamics*, **13**, 321-336.

Nogami, T. and Konagai, K. (1986). "Time Domain Axial Response of Dynamically Loaded Single Piles," *Journal of Engineering Mechanics,* **112**(11), 1241-1252.

Nogami, T. and Konagai, K. (1987). "Dynamic Response of Vertically Loaded Nonlinear Pile Foundations," *Journal of Geotechnical Engineering,* **113**(2), 147-160.

Nogami, T. and Konagai, K. (1988). "Time Domain Flexural Response of Dynamically Loaded Single Piles," *Journal of Engineering Mechanics Division, ASCE* **114**(9), 1512-1525.

Nogami, T., Otani, J., Konagai, K. and Chen, H. L. (1992). "Nonlinear Soil-Pile Interaction Model for Dynamic Lateral Motion," *Journal of Geotechnical Engineering Division, ASCE*, **118**(1), 89-106.

Ottaviani, M. (1975). "Three-Dimensional Finite Element Analysis of Vertically Loaded Pile Groups," *Geotechnique*, **25**(2), 159-174.

Penzien, J. (1970). "Soil-Pile Foundation Interaction," *Earthquake Engineering*, R. L. Wiegel, ed., Prentice-Hall, pp 349-381.

Poulos, H. G. (1989). "Pile Behaviour - Theory and Application," *Geotechnique*, **39**(3), 365-415.

Pressley, J. S. and Poulos, H. G. (1986). "Finite Element Analysis of Mechanisms of Pile Group Behaviour," *International Journal for Numerical and Analytical Methods in Geomechanics*, **10**, 213-221.

Randolph, M. F. (1981). The Response of Flexible Piles to Lateral Loading," *Geotechnique*, **31**(2), 247-259.

Seed, H. B. and Idriss, I. M. (1969). Influence of Soil Conditions on Ground Motions During Earthquake," *Journal of the Soil Mechanics and Foundation Division, ASCE*, **95**(SM1), 99-137.

Trochanis, A. M., Bielak, J., and Christiano, P. (1991a), "Three-Dimensional Nonlinear Study of Piles," *Journal of Geotechnical Engineering,* **117**(3), 429-447.

Trochanis, A. M., Bielak, J., and Christiano, P. (1991b), "Simplified Model for Analysis of One or Two Piles," *Journal of Geotechnical Engineering,* **117**(3), 448-466.

Wolf, J. P. (1985). *Dynamic Soil-Structure Interaction,* Prentice-Hall, Inc. Englewood Cliffs, New Jersey.

Wolf, J. P. (1988). Soil-Structure-Interaction Analysis in Time Domain, in W. J. Hall, ed., "Prentice Hall International Series in Civil Engineering and Mechanics," Prentice-Hall, Inc., Englewood Cliffs, New Jersey.